Gondwana Research xxx (2013) xxx–xxx

Contents lists available at ScienceDirect

Gondwana Research

journal homepage: www.elsevier.com/locate/gr

Detrital and igneous zircon ages for supracrustal rocks of the Kyrgyz Tianshan and palaeogeographic implications

Y. Rojas-Agramonte [a,b,*], A. Kröner [a,b], D.V. Alexeiev [c], T. Jeffreys [d], A.K. Khudoley [e], J. Wong [f], H. Geng [f], L. Shu [g], S.A. Semiletkin [e], A.V. Mikolaichuk [h], V.V. Kiselev [i], J. Yang [j], R. Seltmann [k]

[a] Beijing SHRIMP Centre, Chinese Academy of Geological Sciences, 26 Baiwanzhuang Road, 100037 Beijing, China
[b] Institut für Geowissenschaften, Universität Mainz, D-55099 Mainz, Germany
[c] Geological Institute, Russian Academy of Sciences, Pyzhevsky per. 7, 119017 Moscow, Russia
[d] Imaging and Analysis Centre, Natural History Museum, Cromwell Road, London SW7 5BD, UK
[e] Geological Faculty, St. Petersburg State University, University Embankment 7/9, St. Petersburg 199034, Russia
[f] Department of Earth Sciences, The University of Hong Kong, Pokfulam Road, Hong Kong, China
[g] State Key Laboratory for Mineral Deposits Research, Nanjing University, Nanjing 210093, China
[h] Central Asian Geological–Geophysical Association, Bishkek, Kyrgyzstan
[i] Institute of Geology, Academy of Sciences of Kyrgyzstan, Bishkek 720481, Kyrgyzstan
[j] Institute of Geology and Geophysics, Chinese Academy of Sciences, P.O. Box 9825, Beijing 100029, China
[k] CERCAMS, Department of Earth Sciences, Natural History Museum, Cromwell Road, London SW7 5BD, UK

ARTICLE INFO

Article history:
Received 28 June 2013
Received in revised form 8 September 2013
Accepted 14 September 2013
Available online xxxx

Handling Editor: M. Santosh

Keywords:
Kyrgyzstan
Tianshan
Detrital zircon age
Palaeo-Asian Ocean
Tarim craton

ABSTRACT

We report detrital zircon ages for Precambrian and early Palaeozoic metasediments from the Tianshan orogen in Kyrgyzstan, an important component of the Central Asian Orogenic Belt and compare these with published ages from the Chinese Tianshan and the Tarim craton. These data provide information on possible source terrains and suggest that Precambrian basement is widespread in the Tianshan and may, at least in part, represent continental fragments rifted off the Tarim craton during the early history of the Central Asian Orogenic Belt. Distinct differences in the Precambrian zircon age distribution between the North and Middle Tianshan of Kyrgyzstan support earlier ideas that these two terranes had different crustal histories prior to their amalgamation in the early Palaeozoic. We envisage an archipelago-type scenario for the Palaeo-Asian Ocean south of the Siberian craton in the late Neoproterozoic to early Palaeozoic in which numerous island arcs and Precambrian crustal fragments derived from Tarim drifted northwards (in present coordinates) and were amalgamated and tectonically stacked together during several ocean closure and accretion–collision events. This is surprisingly similar to what has been envisaged for the evolution of Indonesia where Mesozoic rifting of fragments from the Australian margin was followed by Cretaceous collisions and Cenozoic collision of Australia with the SE Asian margin. In both Central Asia and Indonesia continental crust has arrived in the region in multiple episodes and has been fragmented and juxtaposed by subduction-related processes. Continental growth during this process was minimal.

1. Introduction

The Tianshan orogen of Kyrgyzstan, southern Kazakhstan and northwest China is part of the southern Central Asian Orogenic Belt (CAOB) and consists of late Neoproterozoic to Palaeozoic volcano-sedimentary and plutonic arc assemblages that are tectonically interlayered with metamorphic domains, often named complexes. Many of the latter were previously considered to be Archaean or Palaeoproterozoic in age but were shown to be much younger and document high-grade events associated with terrane accretion and subduction during the Palaeozoic (Hegner et al., 2010; Alexeiev et al., 2011; Kröner et al., 2012, 2013). Nevertheless, some Precambrian basement terranes remain and in the Kyrgyz Tianshan were partly characterized by Kröner et al. (2012, 2013) and Konopelko et al. (2008, 2012). There is some speculation on the origin of these Precambrian crustal fragments in the CAOB, and most authors have assumed a Gondwana derivation without being more specific (e.g. Buslov et al., 2001; Dobretsov and Buslov, 2007), whereas Kröner et al. (2012, 2013, in press) from work in the Kyrgyz Tianshan and Rojas-Agramonte et al. (2011) from work in Mongolia concluded that the most likely source is the Tarim craton that now borders the South Tianshan but may originally have been situated close to the northeastern margin of Gondwana (Li et al., 1996; Metcalfe, 2011). This conclusion was primarily based on age similarities of magmatic rocks in the Tianshan, Mongolia and Tarim, notably early Neoproterozoic to late Mesoproterozoic (Grenvillian) ages, as well as

* Corresponding author at: Institut für Geowissenschaften, Johannes Gutenberg-Universität, Becherweg 21 D-55099 Mainz, Germany. Tel.: +49 6131 3920476; fax: +49 6131 3924769.
E-mail address: rojas@uni-mainz.de (Y. Rojas-Agramonte).

1342-937X/$ – see front matter
http://dx.doi.org/10.1016/j.gr.2013.09.005

detrital and xenocrystic zircon age patterns that closely fit the pattern for available zircon ages of the Tarim craton.

In order to further test the hypothesis whether tectonic fragmentation and erosion of the Tarim craton have provided continental material and detritus to build up the accretionary domain of the Tianshan orogen we applied the U–Pb and Lu–Hf methods on detrital zircon grains from sandstones and other metasedimentary rocks in the Kyrgyz Tianshan that are either associated with early Palaeozoic arc terranes or belong to Precambrian tectonic slivers interlayered with the Palaeozoic rocks.

2. Geological outline and tectonic setting of the Kyrgyz Tianshan

The Tianshan thrust-and-fold belt extends for about 2000 km from Uzbekistan to eastern Xinjiang Province of NW China within the southern CAOB (Fig. 1). It represents a complex amalgamation of Palaeozoic island arcs, accretionary complexes and Precambrian micro-continental terranes (Kröner et al., 2012, 2013, in press, and references therein). It evolved during several tectonic episodes from the Neoproterozoic to early Mesozoic, and was reactivated due to uplift and deformation in the late Tertiary and Quaternary (Glorie et al., 2011; De Grave et al., 2013). Tectonically, rocks in the western part of the belt within Uzbekistan and Kyrgyzstan have traditionally been grouped into three major fault-bounded tectonic zones named North Tianshan, Middle Tianshan and South Tianshan, which have distinctly different geological histories and structural patterns (Nikolaev, 1933; Popov, 1938; Bakirov and Maksumova, 2001), which we adopt in this paper.

There is some confusion in the literature on the tectonic nomenclature between the western (former USSR) part of the Tianshan as outlined above and its continuation in northwest China. The Kyrgyz and southern Kazakh North Tianshan is partly equivalent to the Chinese Central Tianshan and partly to what is known as Yili Block in China (Wang et al., 2008), whereas the Kyrgyz Middle Tianshan wedges out near the Kyrgyz–Chinese border and is not present in China (Fig. 1). However, the South Tianshan is equivalent in the west and east although some authors have recently included parts of the previously defined Chinese South Tianshan into the Central Tianshan (e.g., Charvet et al., 2007, 2011). Xiao et al. (2013) also follow the above subdivision and include the Yili Block in the North Tianshan but, like many other Chinese authors, they include into the northwestern part of their North Tianshan rocks that in eastern Kazakhstan are part of the Aktau–Junggar and Balkhash–Yili terranes (Alexeiev et al., 2011). The southern part of the Chinese North Tianshan consists predominantly of volcanic and sedimentary rocks, ranging in age between Early Devonian and early Carboniferous (An et al., in press).

The North Tianshan of Kyrgyzstan and southern Kazakhstan represents one of the oldest orogenic domains in the CAOB and contains large volumes of early Palaeozoic granitoids and is generally characterized by a regional pre-Devonian angular unconformity (Maksumova et al., 2001). On a large scale, it occupies the southern part of two major terranes, namely the Kokchetav–North Tianshan in the center and east, and the Karatau–Talas in the west (see Figs. 1 and 2).

The Kokchetav–North Tianshan consists of Precambrian micro-continental fragments, early Palaeozoic arcs and ophiolite-bearing sutures, as well as high-grade metamorphic domains including HP to UHP rocks, all welded together prior to the Middle Ordovician (see Kröner et al., 2012; Rojas-Agramonte et al., 2013, and references therein). In the Middle to early Late Ordovician the Kokchetav–North Tianshan was dominated by continental arc volcanism (De Grave et al., 2012; Degtyarev et al., 2012), followed by granitoid emplacement in the latest Ordovician and early Silurian (Mikolaichuk et al., 1997; Maksumova et al., 2001; Konopelko et al., 2008; Glorie et al., 2010; Kröner et al., 2012; De Grave et al., 2013).

The Karatau–Talas terrane (Fig. 2) consists of Neoproterozoic to early Palaeozoic low grade greenschists and phyllites, unmetamorphosed Neoproterozoic shallow marine and non-marine siliciclastic sediments with subordinate felsic tuffs, and Cambrian to Middle Ordovician carbonates (Cook et al., 1991; Maksumova et al., 2001; Meert et al., 2011). It may either represent an independent microcontinent, wedged between the Kokchetav–North Tianshan and the Middle Tianshan (Maksumova et al., 2001), or constitutes the marginal part of the Middle Tianshan microcontinent that was affected by deformation and intruded by granites in the Late Ordovician during collision with the Kokchetav–North Tianshan (Kröner et al., 2013 and references therein).

The Kyrgyz Middle Tianshan represents the southern part of the larger Ishim–Middle Tianshan microcontinent that extends from the Tianshan to the western part of northern Kazakhstan (Avdeev and Kovalev, 1989; see Fig. 6 in Windley et al., 2007). It most likely constitutes a single coherent continental block, about 2000 km long. The oldest rocks are amphibolite-facies metasediments and orthogneisses of the Kuilyu Complex in the Sarydjaz River basin in the far eastern part of the Middle Tianshan (Fig. 1), that yielded Palaeoproterozoic zircon ages of 2.3 to 1.7 Ga (Kiselev et al., 1982, 1993; Glorie et al., 2011; Kröner et al., 2013). Neoproterozoic granites and felsic volcanic rocks are common within the entire Ishim–Middle Tianshan microcontinent from eastern Kyrgyzstan to central Kazakhstan (Kiselev et al., 1993; Kröner et al., 2009; Glorie et al., 2011; Kröner et al., 2013). The Precambrian basement rocks are overlain unconformably by late Neoproterozoic

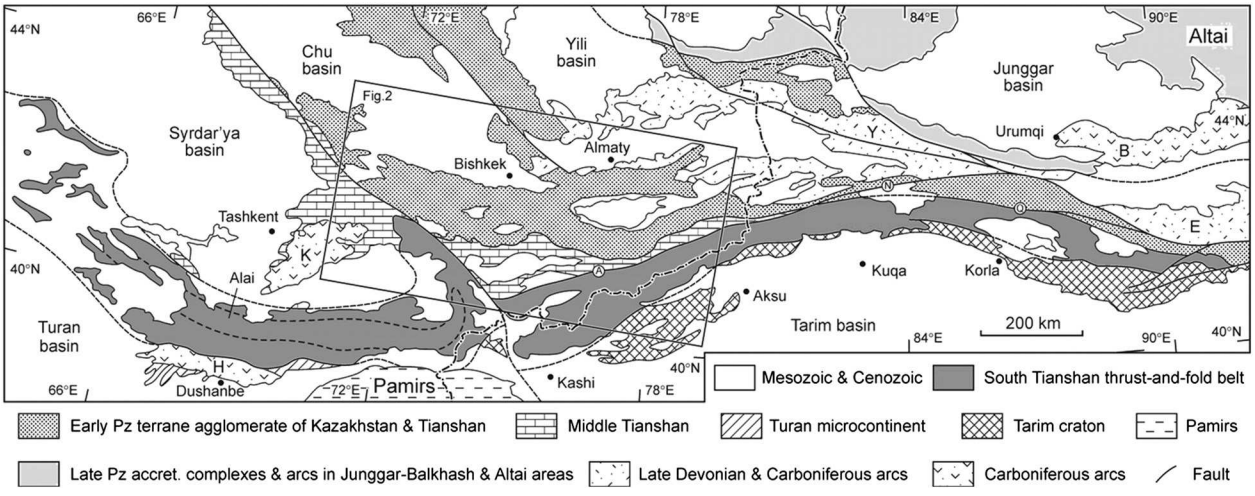

Fig. 1. Overview map of the Tianshan mountain range showing major tectonic subdivisions. Abbreviated names: Continental arcs: Y — Yili, E — East Tianshan, H — Hissar, K — Beltau-Kurama, B — Bogdoshan. Major faults: A — Atbashi — Enylchek, N — South Nalati, Q — Qavabulak. Dashed line is boundary between China and countries of the former Soviet Union. Modified after Biske et al. (2012).

Please cite this article as: Rojas-Agramonte, Y., et al., Detrital and igneous zircon ages for supracrustal rocks of the Kyrgyz Tianshan and palaeogeographic implications, Gondwana Research (2013), http://dx.doi.org/10.1016/j.gr.2013.09.005

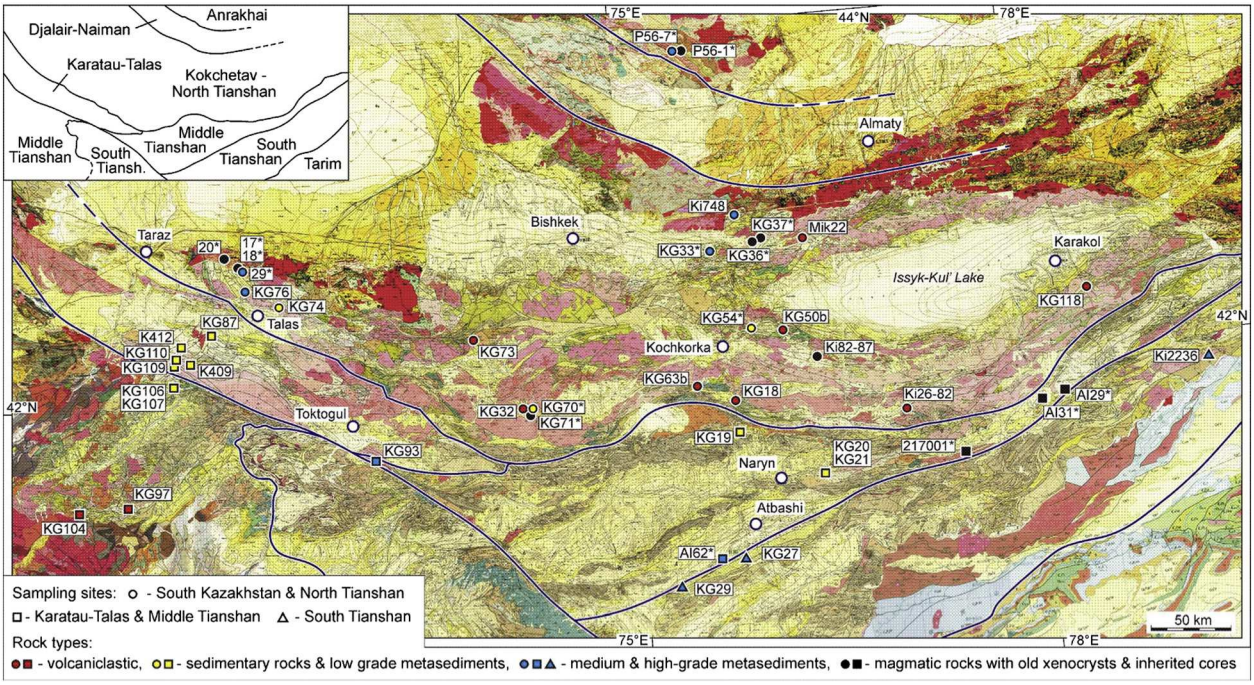

Fig. 2. Geological map of the Tianshan within Kyrgyzstan, southern Kazakhstan and northwestern China showing tectonic subdivision and location of samples analyzed in this study and discussed in the text. Sample numbers with asterisk are from Alexeiev et al. (2011), Glorie et al. (2011), Seltmann et al. (2011), Konopelko et al. (2012), Kröner et al. (2007, 2012, 2013, in press). Other samples — this study. Base map compiled from Chakabaev (1979), Osmonbetov (1980), Shayakubov (1998), and Li and Xu (2007).

rift-related subalkaline basalts and rhyolites, diamictites and shales, cherts, carbonates and turbidites (Ankinovich, 1961; Osmonbetov et al., 1982; Maksumova et al., 2001). A general feature of the Middle Tianshan is a lack of early Palaeozoic granitoids and a weakly developed Late Ordovician angular unconformity (Osmonbetov et al., 1982).

The South Tianshan is a late Palaeozoic accretionary and collisional thrust-and-fold belt and consists mainly of middle to late Palaeozoic marine sedimentary rocks, subordinate ophiolites, and metamorphic rocks, that are imbricated and stacked together along major mainly south-facing thrusts, thus suggesting N-directed subduction during the accretion–collision process (Biske, 1995, 1996; Biske et al., 2012). Recent papers indicate an important phase of late Palaeozoic granitoid magmatism in the South Tianshan (Konopelko et al., 2007; Glorie et al., 2011; Seltmann et al., 2011; De Grave et al., 2012).

Our samples are distributed over a large area within the North and Middle Tianshan, with few samples from the South Tianshan. Their locations are shown in Fig. 2 and Table 1 that also provide information on the lithology and regional stratigraphy. Several samples from the Tianshan of southern Kazakhstan, namely the Chu–Yili Mountains (Kröner et al., 2007; Alexeiev et al., 2011) and the Karatau Range (Levashova et al., 2011) are also included in our age assessment.

3. Results

We undertook single zircon dating of detrital, magmatic and xenocrystic grains, and in view of the different laboratories involved the data are shown in separate tables (S1–S6) listed in a separate file named "Supplementary material" and available from the Publisher on request. We used the laser-ablation ICP-MS in laboratories of the Natural History Museum, London, UK (Table S1), the Dept. of Geosciences, University of Mainz, Germany (Table S2), and the Department of Earth Sciences, University of Hong Kong, China (Table S3). In addition, zircon grains from several samples were dated on SHRIMP II instruments in the Beijing SHRIMP Centre, Chinese Academy of Sciences (Table S4), and the Centre of Isotopic Research, VSEGEI, St. Petersburg, Russia (Table S5). Selected grains from several samples were also analyzed for Hf-in-zircon isotopes in the Institute of Geology and Geophysics, Chinese Academy of Sciences, Beijing (Table S6), and a summary of the data is shown in Fig. 3. The analytical procedures are summarized in the Appendix A. The analyses were performed on mounts where the zircon grains were approximately sectioned in half to expose their interiors, and analytical spots were selected on the basis of cathodoluminescence (CL) images. Precise dating of young zircon crystals (<1000 Ma) is best achieved by using concordant $^{206}Pb/^{238}U$-ages, whereas older grains are more precisely dated using $^{207}Pb/^{206}Pb$ ages. This is because old grains with larger amounts of radiogenic Pb are more reliably assessed by $^{207}Pb/^{206}Pb$ ages. As the age decreases the amount of radiogenic lead available for measurement also decreases, which results in higher errors in the $^{207}Pb/^{206}Pb$ age. Therefore, for younger grains, the $^{206}Pb/^{238}U$ age is generally more precise but only provides reliable geological information if the analysis is concordant (Sircombe, 1999; Black et al., 2003).

Most detrital zircon grains are mechanically rounded due to sedimentary transport, and this may vary from only little abrasion at the pyramidal terminations to almost spherical grains (e.g., Fig. S2c). Most likely, the subrounded and near-euhedral grains experienced rather short transport, and their source areas are not far from the depositional sites. This is well documented in several samples where the ages reveal only one zircon population. Samples with highly variable detrital zircon morphologies and colors generally have more variable ages, reflecting multiple zircon source areas. Extensively rounded grains often, but not always, reveal the oldest ages. It is very difficult to specify the source areas of most old grains because many may be derived from second or third-cycle sediments, and the original source is now impossible to identify. Therefore, the interpretation of some of the old ages remains somewhat speculative.

On the basis of their age patterns, our samples can be divided into two groups. One group consists of zircon populations with a rather uniform morphology and unimodal age distributions, whereas the other group has highly diverse morphologies and ages. In view of the geological entities encountered in the North and Middle Tianshan and their field relationships it is likely that the first group reflects sediments intimately associated with Palaeozoic island arc evolution. This is confirmed by some of the host sediments that are interlayered with arc volcanic rocks. Sediments reflecting more variable zircon ages are

Please cite this article as: Rojas-Agramonte, Y., et al., Detrital and igneous zircon ages for supracrustal rocks of the Kyrgyz Tianshan and palaeogeographic implications, Gondwana Research (2013), http://dx.doi.org/10.1016/j.gr.2013.09.005

Table 1
Summary of lithologies, locations and age ranges for magmatic, detrital and xenocrystic zircons in rocks of the Kyrgyz–Kazakh Tianshan.

Sample no.	N. Lat. E. Long.	Area, locality	Formation (F.) Complex (C.)	Rock type (stratigraphic position)	Magmatic age () or age range (Ma)	Method, laboratory	Reference
Kyrgyz North Tianshan and southern Kazakhstan							
17	42°46.22′ 72°04.36′	West Kyrgyz Range, NW of Talas	Makbal C.	Eclogite	577–1375	SHRIMP II, VSEGEI	Konopelko et al. (2012)
18	42°46.20′ 72°04.45′	West Kyrgyz Range, NW of Talas	Makbal C.	Eclogite	505–1915	SHRIMP II, VSEGEI	Konopelko et al. (2012)
20	42°49.14′ 71°56.4′	West Kyrgyz Range, NW of Talas	Kandjailyau C.	Granitic gneiss	509–1479	SHRIMP II, VSEGEI	Konopelko et al. (2012)
29	42°46.19′ 72°04.50′	West Kyrgyz Range, NW of Talas	Makbal C.	UHP schist	513–1843	SHRIMP II, VSEGEI	Konopelko et al. (2012)
KG18	41°53′31.8″ 75°43′ 45.7″	North of Dolon Pass	Karadjorgo F.	Sandstone	463–485	ICPMS, Mainz	This study, Table S3
KG32	41°55′24.6″ 74°10′ 21″	Susamyr Range, Kokomeren R.	Unnamed	Tuff layer	(511) 1727–2445	SHRIMP II, Beijing	This study, Table S4
KG33	42°42′49.2″ 75°37′ 01.2″	East Kyrgyz Range, south of Orlovka	Kemin C.	Migmatitic paragneiss	503–1263	SHRIMP II, Beijing	Kröner et al. (2012)
KG36	42°46′17.1″ 75°57′ 52.0″	West Trans-Yili Range, Kemin area	Kemin C.	Migmatite	(799) 1180	SHRIMP II, Beijing	Kröner et al. (2012)
KG37	42°48′12.1″ 76°01′ 32.8″	West Trans-Yili Range, Kemin area	Dolpran C.	Granite	(472) 783	SHRIMP II, Beijing	Kröner et al. (2012)
KG50b	42°15′07.1″ 76°09′ 38.5″	Tegerek Range SW of Issyk-Kul	Karadjorgo F.	Tuff–sandstone	(~493)	ICPMS, London	This study, Table S1
KG54	42°16′20.7″ 75°51′ 15.5″	East of Kochkorka	Senkeltey C.	Quartzite (PR_2)	1168–1615	ICPMS, HKU	Kröner et al. (2012)
KG63b	41°57′53.3″ 75°26′ 34.7″	South Karakatty Range, N of Sonkul	Choloi F.	Tuff–sandst.	(485) 545–560	ICPMS, HKU	This study, Table S2
KG70	41°54′30.6″ 74°16′ 17.9″	Susamyr Range, Kokomeren R.	Turagain C.	Granite	(1129) 1563–2001	SHRIMP II, Beijing	Kröner et al. (2013, in press)
KG71	41°54′30.6″ 74°16′ 17.9″	Susamyr Range, Kokomeren R.	Turagain C.	Biotite paragneiss (PR_2)	1164–1250	SHRIMP II, Beijing	Kröner et al. (2013, in press)
KG73	42°19′42.6″ 73°49′ 05.9″	Kyrgyz Range, Tyu-Ashuu Pass	Unnamed	Tuff–sandstone	(465) 950–1900	ICPMS, London	This study, Table S1
KG74	42°33′38.2″ 72°22′ 10.5″	South Kyrgyz Range, east of Talas	Ortotau C.	Sandstone (PR_2)	1170–2920	ICPMS, London	This study, Table S1
KG76	42°39′06.9″ 72°05′ 52.4″	South Kyrgyz Range, NW of Talas	Makbal C.	Quartzite	1810–3810	ICPMS, London	This study, Table S1
KG118	42°17′59.3″ 78°29′ 08.9″	East Terskey Range, Karak\ol River	unnamed	Cherty siltstone	1000–2800	ICPMS, London	This study, Table S1
Ki748	42,92917° 75,85897°	Trans-Yili Range, west of Aktyuz	Kemin C.	Migmatitic paragneiss	787–2460	SHRIMP II, Beijing	This study, Table S4
Ki2682	41°45′22.8″ 77°01′ 15.8″	Central Terskey Range, Burkhan R.	unnamed	Hbl. gneiss	(494)–685	SHRIMP II, Beijing	This study, Table S4
Ki8287	42.1517° 76.26408°	West Terskey Range	Susamyr C.	Monzodiorite	(435) 478–1637	SHRIMP II, Beijing	This study, Table S4
KZ26	–	Chu–Yili Mts., Sulusai area	Sulusai F.	Siltstone (Cm)	2228–2425	Evaporation, Mainz	Kröner et al. (2007)
KZ23	–	Chu–Yili Mts., Sulusai, Kopakty River	Djambul F.	Sandstone (O_1)	(490) 2038–2782	Evaporation, Mainz	Kröner et al. (2007)
KZ39	–	Chu–Yili Mts., SW of Lake Balkhash	Kotnak C.	Granodiorite	(480) 548–2288	Evaporation, Mainz	Kröner et al. (2007)
KZ42	–	Chu–Yili Mts., SW of Lake Balkhash	Unnamed	Metadacite	(478) 843	Evaporation, Mainz	Kröner et al. (2007)
P56/1	43°53′40.1″ 75°27′ 46.6″	South Chu–Yili Mts., Anrakhai area	Unnamed	Granodiorite	(509) 927–1214	SHRIMP II, Beijing	Alexeiev et al. (2011)
P56/7	43°53′36.5″ 75°27′ 43.2″	South Chu–Yili Mts., Anrakhai area	Anrakhai C.	Garnet–Musc.–schist	694–2557	ICPMS, HKU	Alexeiev et al. (2011)
Mik22	42°45′39.6″ 76°23′ 30.7″	North Kungey Range, Tuyuk R.	Karakorum F.	Dacitic tuff	(489) 833–1123	SHRIMP II, Beijing	This study, Table S4
Middle Tianshan and Karatau–Talas terrane							
KG19	41°41′37.9″ 75°44′ 14.9″	South Moldotau Range, Naryn area	Ichkebash F.	Sandstone (O_3)	758–2355	ICPMS, Mainz	This study, Table S3
KG20	41°27′02.2″ 76°17′ 57.3″	Naryn River east of Naryn	Djetymtau F.	Dacite clast	(836) 2340	SHRIMP II, Beijing	This study, Table S4
KG21	41°26′51.2″ 76°17′ 16.0″	Naryn River east of Naryn	Djetymtau F.	Sandstone (PR_3)	629–2345	ICPMS, Mainz	This study, Table S3
KG87	42°25′00″ 71°50′17″	Talas Range, Kumyshtag R.	Sarydjon F.	Sandstone	873–2600	ICPMS, HKU	This study, Table S2
KG93	41°40′48.7″ 72°59′ 59.7″	Toktogul area, Karasu R.	Takhtalyk C.	Paragneiss	695–1900	ICPMS, London	This study, Table S1
KG97	41°26′10.3″ 71°13′ 43.5″	South Chatkal Range, Kasansay River	Semizsai C.	Chlorite–Albite–schist	(~460)	ICPMS, London	This study, Table S1
KG104	41°27′38.1″ 70°56′ 17.3″	South Chatkal Range, Ishtamberdy R.	Semizsai C.	Biotite–Musc.–schist	(460) 510–3000	ICPMS, London	This study, Table S1
KG106	42°07′47.0″ 71°33′ 26.5″	South Talas Range, Karakysmak R.	Shorashu F.	Granite clast	1804–1927	SHRIMP II, Beijing	This study, Table S4
KG107	42°08′07.8″ 71°33′ 12.5″	South Talas Range, Karakysmak R.	Shorashu F.	Sandstone (PR_3)	1800–2880	ICPMS, London	This study, Table S1
KG109	42°17′25.5″ 71°34′ 37.3″	Talas Range, Karabura River	Karabura F.	Sandstone	860–2770	ICPMS, London	This study, Table S1
KG110	42°18′38.0″ 71°35′ 30.5″	Talas Range, Karabura River	Kyzylbel F.?	Sandstone	820–2700	ICPMS, London	This study, Table S1

Please cite this article as: Rojas-Agramonte, Y., et al., Detrital and igneous zircon ages for supracrustal rocks of the Kyrgyz Tianshan and palaeogeographic implications, Gondwana Research (2013), http://dx.doi.org/10.1016/j.gr.2013.09.005

Table 1 (*continued*)

Sample no.	N. Lat. E. Long.	Area, locality	Formation (F.) Complex (C.)	Rock type (stratigraphic position)	Magmatic age () or age range (Ma)	Method, laboratory	Reference
Middle Tianshan and Karatau–Talas terrane							
K409	42°15′50″ 71°42′27″	Talas Range, Kumyshtag River	Kyzylbel F.?	Sandstone	661–2995	SHRIMP II, VSEGEI	This study, Table S5
K412	42°25′36″ 71°34′27″	Talas Range, Karabura River	Tagyrtau F.	Sandstone	757–2544	SHRIMP II, VSEGEI	This study, Table S5
AI29	41°42′53″ 78°09′49″	Akshiyryak Range, Karasai valley	Sarydjaz C.	Migmatite	(806) 1400–2324	ICPMS, Ghent	Glorie et al. (2011)
AI31	41°44′12″ 78°03′59″	Djetymbel Range, Arabel Pass	Great Naryn F.	Felsic tuff	(842) ~2060	ICPMS, Ghent	Glorie et al. (2011)
AI62	~41°01′ 75°34′	North Atbashi Range, Kazybek village	Kembel C.	Schist (PZ_1?)	788–2441	ICPMS, Ghent	Glorie et al. (2011)
217001	41.4647° 77.4411°	East Naryntau Range	Ulan pluton	Granite	(303) 998	SHRIMP II, VSEGEI	Seltmann et al. (2011)
South Tianshan							
KG25	–	North Atbashi Range, Kembel River	Atbashi C.	Paragneiss (PZ_2)	830–2527	SHRIMP II, Beijing	Hegner et al. (2010)
KG25	–	North Atbashi Range, Kembel River	Atbashi C.	Paragneiss (PZ_2)	427–2774	ICPMS, Mainz	Hegner et al. (2010)
KG25		North Atbashi Range, Kembel River	Atbashi C.	Paragneiss (PZ_2)	403–2645	ICPMS Mainz	This study, Table S3
KG27	–	North Atbashi Range, Kembel River	Atbashi C.	Paragneiss (PZ_2)/12	403–932	ICPMS, Mainz	This study, Table S3
KG29	40°52′49.1″ 75°16′ 04.0″	North Atbashi Range, Tashrabat River	Atbashi C.	Paragneiss (PZ_2)/25	329–2620	ICPMS, Mainz	This study, Table S3
Ki2236	41°44′20,8″ 79°08′ 30,6″	East Kokshaal Range, Sarydjaz area	Choloktor C.	Micaschist (PZ_2)/60	600–3450	ICPMS, London	This study, Table S1

most likely derived from Precambrian sources, either from continental fragments that abound in the Tianshan (e.g., Kröner et al., 2012, 2013, in press) or elsewhere in the CAOB (Kozakov et al., 2007; Rojas-Agramonte et al., 2011; Rytsk et al., 2011) or from cratonic domains such as Tarim (Kröner et al., 2012; Ma et al., 2012a,b; Kröner et al., 2013) that supplied detritus into the Palaeo-Asian Ocean. However, some samples providing Palaeozoic as well as Precambrian ages most likely have a mixed origin and are partly derived from arc terranes and partly from continental protoliths.

We first present the results for individual samples by region and discuss the relevance of the detrital and xenocrystic zircon ages for the origin of these rocks. In several cases we also discuss published data for similar rocks or associations as our samples. Concordia diagrams of the dated samples, including representative CL-images of dated zircon grains, are shown in the Supplementary material that is available from the publisher on request. The diagrams showing LA-ICP-MS data are all included in Fig. S1, whereas the SHRIMP data of the Beijing laboratory are shown in Fig. S2 and those of the VSEGEI laboratory in Fig. S3. Hf-in-zircon isotopic data are shown in the Hf evolution diagrams of Fig. S3.

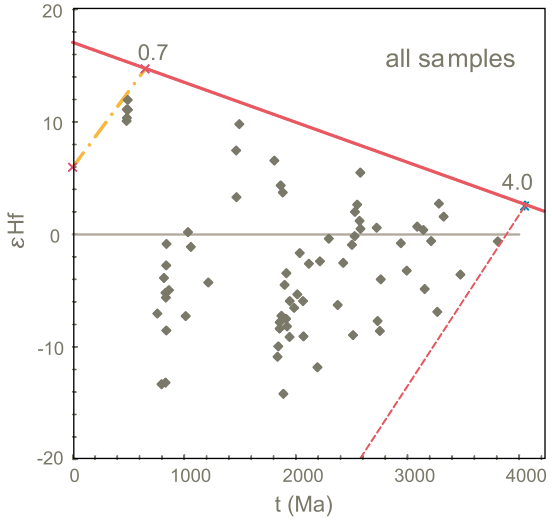

Fig. 3. Composite Hf evolution diagram for detrital zircons of the Kyrgyz North Tianshan. For details on individual samples see Table S6. The solid red line is the depleted mantle evolution line after Griffin et al. (2000). The two dashed lines indicate the evolution of the $^{176}Lu/^{177}Hf$ ratios for the youngest and oldest zircons measured, respectively. The slopes are based on a mean crustal $^{176}Lu/^{177}Hf$ ratio of 0.01 (see Kröner et al., in press) for explanation. (For interpretation of the references to color in this figure legend, the reader is referred to the web version of this article.)

We have combined our data, together with published zircon ages, into general age spectra (probability plots) for the Kyrgyz Tianshan and compare these with similar plots for data available for the Chinese Central Tianshan (including Yili Block) and the Tarim craton. These spectra are shown in Fig. 4. The data for these plots are based on Excel spreadsheets that are available as Supplementary files in Tables S7–S9. Finally, we speculate on the significance of the age patterns for the evolution of the CAOB.

3.1. Kyrgyz North Tianshan

Our study in the North Tianshan and adjacent southern Kazakhstan included a variety of rock types that we grouped in the following manner: a) Mesoproterozoic metasediments that represent a sedimentary cover of the Palaeoproterozoic basement of the North Tianshan microcontinent, b) Proterozoic and early Palaeozoic meta-sedimentary rocks within Early Ordovician medium- and high-grade metamorphic complexes, c) early Palaeozoic arc-related sequences, d) Xenocrystic zircon grains and old cores in Mesoproterozoic and Palaeozoic rocks of magmatic origin.

3.1.1. Mesoproterozoic metasediments

Mesoproterozoic metasediments represent the oldest proven rocks in the North Tianshan and have been interpreted as a sedimentary cover of the Palaeoproterozoic North Tianshan microcontinent (Mitrofanov, 1982; Ghes, 2008). They consist of marble, biotite schist and subordinate metasandstone and are mainly exposed in the Talas and Kochkorka areas and were included in the Ortotau and Senkeltey Complexes, respectively. The sequences also include Mesoproterozoic stromatolites and are cut by ~1.1 Ga old granites (Kröner et al., 2013, in press and references therein).

Sample KG74 is a mature sandstone collected from the Ortotau Complex in the western North Tianshan, some 10 km east of Talas (Table 1, Fig. 2). The zircon grains are well rounded, most are oval-shaped to spherical and display well-preserved oscillatory zoning (Fig. S1k, inset). The morphology suggests long or repeated sedimentary transport, a typical feature of many Precambrian detrital grains, and this is confirmed by the isotopic data. Forty-eight grains were analyzed and provided mostly concordant results (Table S1) with ages ranging from ca. 1170 to 2920 Ma (Fig. S1k). There are only a few grains with Mesoproterozoic ages up to ca. 1500 Ma, and most analyses are spread along the Concordia curve between 1700 and 2100 Ma (Fig. S1k). Archaean ages constitute a distinct group and range from 2500 to 2920 Ma. The previously assumed Precambrian depositional age is supported by the above zircon age distribution, suggesting deposition at less than 1170 Ma.

Please cite this article as: Rojas-Agramonte, Y., et al., Detrital and igneous zircon ages for supracrustal rocks of the Kyrgyz Tianshan and palaeogeographic implications, Gondwana Research (2013), http://dx.doi.org/10.1016/j.gr.2013.09.005

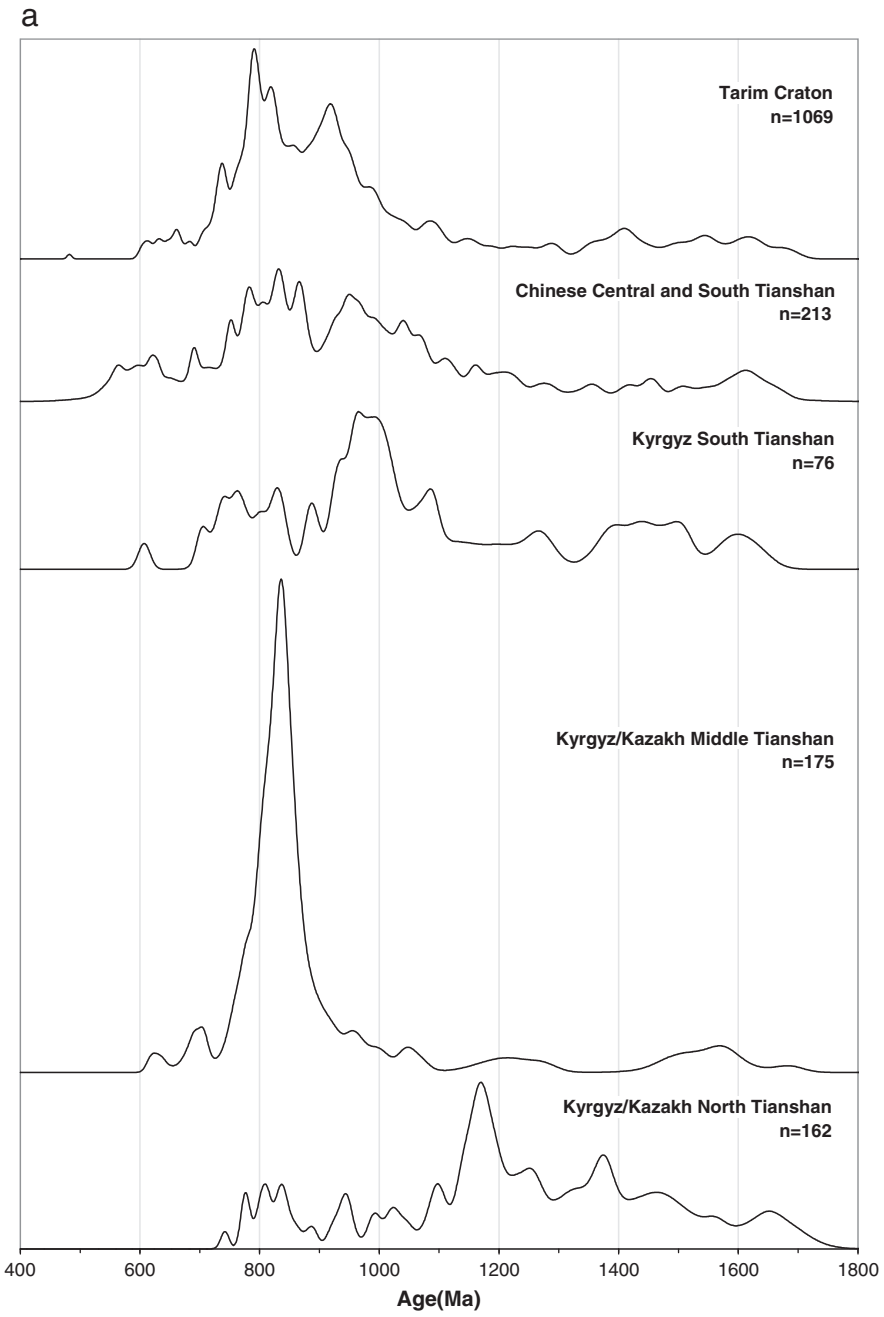

Fig. 4. Probability plots of zircon ages >600 Ma for rocks from the Kyrgyz and southern Kazakh North Tianshan, the Kyrgyz Middle Tianshan, the Chinese Centrial & South Tianshan, Yili Block, and the Tarim craton. (a) Time period 500–1800 Ma; (b) time period 1500–4000 Ma. Inset in Fig. 4b shows detrital zircon ages for sample Ki2236, time period 1500–4000 Ma. For data and references see Tables S1–S5 and S7–S9.

Ages for samples from the same suite were previously reported by Kröner et al. (2013, in press) and include a quartzite from the Senkeltey Complex near Kochkorka (KG54) and a biotite paragneiss xenolith from a Mesoproterozoic granite on the Kökömeren River (KG71). Both samples contain numerous detrital zircon grains with most analyses spread along Concordia from 1168 to 1615 Ma in KG54 and 1164 to 1250 in KG71 (see Kröner et al., 2013 for details).

3.1.2. Proterozoic and early Palaeozoic metasediments within Ordovician metamorphic complexes

Proterozoic and early Palaeozoic metasediments within Ordovician metamorphic complexes are known from the Makbal and Aktyuz areas of the North Tianshan and the Anrakhai area of southern Kazakhstan. In the older literature these rocks were assumed to be Archaean to Palaeoproterozoic in age (Bakirov and Maksumova, 2001). However Neoproterozoic and early Palaeozoic ages have recently been obtained for most rock types by single zircon dating. The rocks underwent medium- to high-grade metamorphism in an accretionary and collisional setting during the early Ordovician at ~490–475 Ma (Alexeiev et al., 2011; Konopelko et al., 2012; Kröner et al., 2012; Rojas-Agramonte et al., in press).

Sample KG76 is from the southern part of the Makbal metamorphic terrane in the western North Tianshan and represents a micaceous quartzite that occurs as a tectonic boudin in a strongly deformed sequence of schists of uncertain age (Fig. 2). The block may be derived from the Makbal unit that is exposed in the core of an antiform to the north where similar rocks occur (Bakirov, 1978; Konopelko et al., 2012 and references therein). The zircon grains are perfectly rounded

Please cite this article as: Rojas-Agramonte, Y., et al., Detrital and igneous zircon ages for supracrustal rocks of the Kyrgyz Tianshan and palaeogeographic implications, Gondwana Research (2013), http://dx.doi.org/10.1016/j.gr.2013.09.005

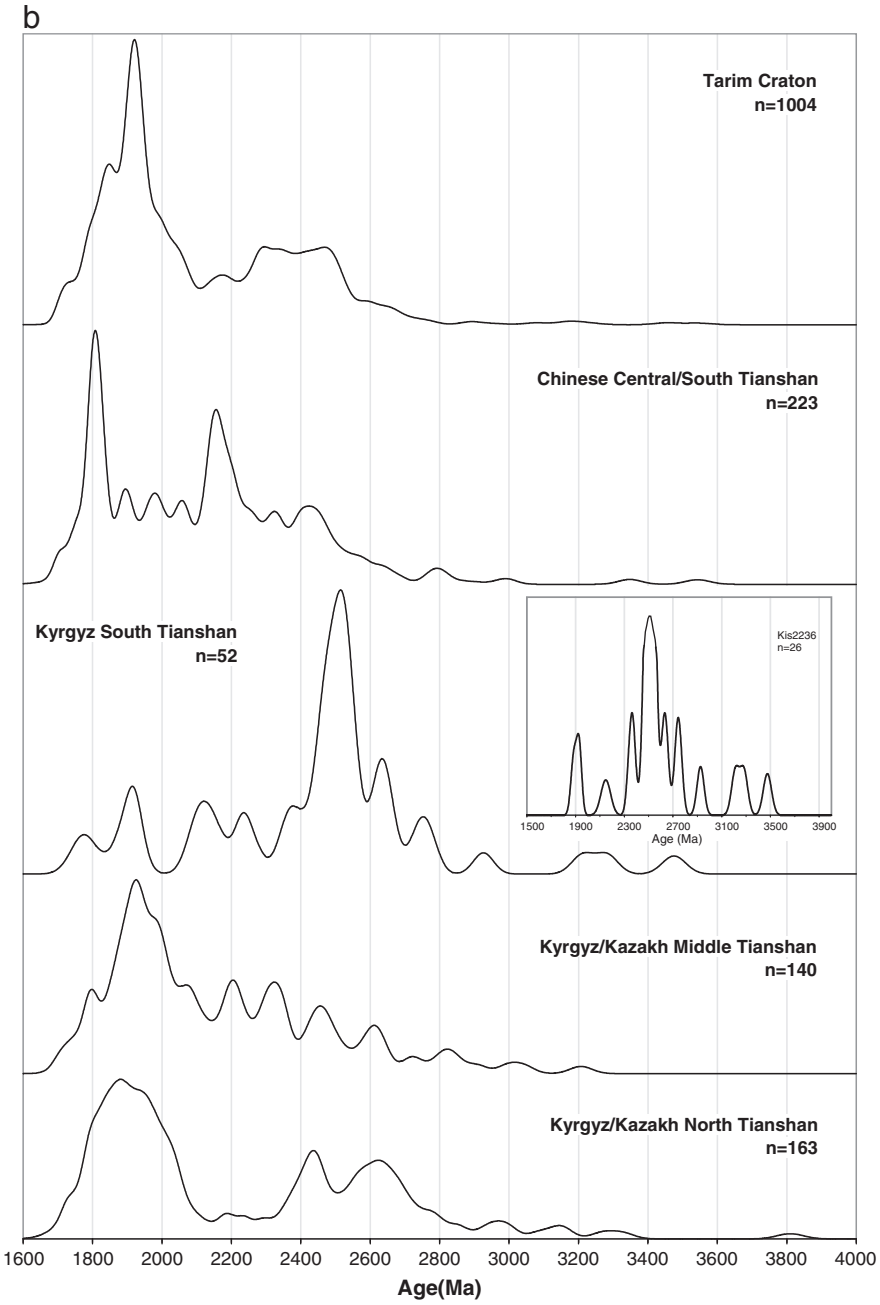

Fig. 4 (*continued*).

and have oval to spherical shapes and highly variable CL images (Fig. S1l, inset). Seventy-two grains were analyzed and provided an array of concordant or near-concordant data corresponding to ages between ca. 1730 and 3780 Ma (Table 2, Fig. S1l). Most ages straddle the Concordia curve with a strong grouping between 1900 and 2000 Ma and almost continuously older ages up to 2900 Ma (Fig. S1l). Then there is a short break and another, smaller, group is defined by ages between 2980 and 3300 Ma. Finally, one single, spherical grain yielded the oldest age yet reported for any rock from the Tianshan, namely 3770 Ma (Table 2, Fig. S1l). This age distribution suggests that this sample was deposited in the Precambrian, and the zircon grains reflect a diverse source area composed of Palaeoproterozoic to early Archaean rocks. The most likely source is the Tarim craton as we shall discuss below. Detrital zircon ages ranging from 598 to 1875 Ma were also reported in the same area from a metasedimentary UHP garnet–talk–chloritoid schist (Konopelko et al., 2012).

Two samples were collected from the Kemin Complex in the Aktyuz area, previously considered to be Palaeoproterozoic in age (Kiselev et al., 1993). Sample Ki748 is from a feldspar-rich layer in a migmatitic paragneiss collected at the western termination of the Trans-Yili Range, some 23 km west of Aktyuz (Table 1, Fig. 2). The zircon crystals are mainly oblong to oval-shaped and display variable degrees of rounding. The CL images reveal simple as well as complex internal textures, including metamictization and recrystallization. Some grains have extremely thin high luminescence (low-U) rims, probably reflecting metamorphic overgrowth. Nine grains were dated on SHRIMP II, and the concordant ages range from 787 ± 10 to 1380 ± 9 Ma, whereas one discordant analysis suggests an early Palaeoproterozoic age of 2460 ± 5 Ma (Table 3, Fig. S2c). The limited data are not sufficient to assess the likely depositional age of the gneiss protolith, which must be Neoproterozoic or younger, but a chronologically mixed Precambrian source is indicated.

Please cite this article as: Rojas-Agramonte, Y., et al., Detrital and igneous zircon ages for supracrustal rocks of the Kyrgyz Tianshan and palaeogeographic implications, Gondwana Research (2013), http://dx.doi.org/10.1016/j.gr.2013.09.005

Sample KG33 is a migmatitic paragneiss of presumed Precambrian age, collected south of Orlovka at the eastern termination of the Kyrgyz Range (Table 1, Fig. 2), and the field relationships and zircon geochronology have been described by Kröner et al. (2012). Seven concordant grains dated on SHRIMP II are certainly not representative of the detrital population, but the youngest zircon at 503 ± 8 Ma shows this rock to be younger than middle Cambrian and not Proterozoic. The older grains from 773 ± 6 to 1263 ± 10 Ma are in the same range as previous samples.

Finally, sample P56-7 is a garnet mica–schist collected from a HP metamorphic unit in the Anrakhai area of the southern Chu–Yili Mountains in Kazakhstan, and the geology and detrital zircon ages were presented by Alexeiev et al. (2011). The rock contains well-rounded detrital grains, and 16 SHRIMP-dated grains yielded concordant ages ranging from 694 ± 7 to 2557 ± 27 Ma.

3.1.3. Arc-related volcano-sedimentary sequences

Arc-related volcano-sedimentary sequences are extensively developed in the North Tianshan, and palaeontological and isotopic data indicate that they range in age from Neoproterozoic(?) and Cambrian to Late Ordovician (Mikolaichuk et al., 1997; Kröner et al., 2012), though many formations remain poorly dated.

The oldest presumably arc-related rock was dated SE of Lake Issyk-Kul. Sample KG118 is a thinly laminated cherty siltstone from an unnamed sequence and was collected on the Terskey Range along the Karakol River (Table 1, Fig. 2). The zircon crystals are mostly equant and well rounded and display variable textures in CL with some revealing core–rim structures (Fig. S1t, inset). Thirty-six grains were dated (Table 2), and the concordant results reflect a chronologically extremely heterogeneous source with ages ranging from just over 1000 to 2800 Ma (Fig. S1t). Here again a Neoproterozoic age of deposition is likely, and the source terrane ranges in age from Mesoproterozoic to Archaean.

Early Cambrian volcanic rocks, exposed on the Kokomeren River in the Susamyr Range, contain green laminated tuff (sample KG32, Table 1, Fig. 2) that forms interlayers in light-colored shallow-marine limestone. The sample contains magmatic zircon grains, dated on SHRIMP, with a mean $^{206}Pb/^{238}U$ age of 511 ± 4 Ma as well as much older xenocrystic or detrital grains with Paleoproterozoic ages of 1727 and 2445 Ma (Table 2, Fig. S2b). The 511 age corresponds well with zircon ages for granites in the same region (Glorie et al., 2010).

Two samples of arc-related rocks from the Karadjorgo Formation were dated, one from the northern slope of Dolon Pass (KG18) and another from the Tegerek Range southwest of Lake Issyk-Kul (KG50b). The age of this formation is well constrained within late Cambrian to early Floian (Early Ordovician) in the Dolon area by conodonts occurring in chert interlayers (Mikolaichuk et al., 1997 and references therein). In other places the age of the rocks which are conditionally related to the same formation is unknown due to the lack of fossils, and possible correlation is therefore ambiguous.

Sample KG18 is an arc-derived turbiditic sandstone collected north of the Dolon Pass (Table 1, Fig. 2). The zircon crystals are variably long- or short-prismatic, clear, euhedral or very little rounded at their pyramidal terminations and most grains reveal excellent oscillatory zoning (Fig. S1a, inset). The similarity on their CL-images clearly show these grains to belong to a single magmatic population, and this is also confirmed by the isotopic data (Table S2), defining a well grouped pattern reflecting 24 analyses in the Concordia diagram and a Concordia age of 475.2 ± 1.4 Ma (Fig. S1a). We interpret this age to reflect arc magmatism in the early Floian (early Ordovician).

Sample KG50b is a green tuff–sandstone interlayered with metavolcanic rocks on the northern slope of the Tegerek Range SW of Lake Issyk-Kul (Table 1, Fig. 2). The zircon crystals are clear, perfectly euhedral and display excellent oscillatory zoning (Fig. S1g, inset), showing them to belong to one genetic population. Thirty-five zircon grains were analyzed (Table 2) and provided a well-grouped set of isotopic ratios with a mean Concordia age of 492.6 ± 1.6 Ma (Fig. S1g). There is no doubt that these grains are derived from a late Cambrian magmatic sequence and thus date arc volcanic activity in this region. This is supported by Cambrian crystallization ages for dolerites from Dolon Pass (Glorie et al., 2010), suggesting that arc magmatism began in the Cambrian.

Sample KG63B is a medium-grained tuff–sandstone of the Choloi Formation (Lomize et al., 1997; Mikolaichuk et al., 1997 and references therein) and was collected on the southern slope of the Karakatta Range north of Sonkul (Table 1, Fig. 2). The zircon crystals are mostly euhedral with few showing slight rounding at their terminations, and the CL images are distinctly more variable in their internal textures than in the samples of Section 3.1 (Fig. S1i, inset). Twenty-one grains were analyzed (Table S3) and provided an array of concordant data with a cluster at 485 Ma and older ages extending to ca. 560 Ma (Fig. S1i). We suggest that the youngest cluster represents arc-derived zircon grains reflecting early Ordovician volcanic activity at Karakatta Range, whereas slightly older grains with overlapping ages may reflect earlier volcanic activity during the same volcanic event. The two oldest grains at ca. 545 and 560 Ma are probably derived from a slightly older late Neoproterozoic source such as the eastern part of the Kyrgyz Terskey zone where arc-related volcanic rocks with such ages have been inferred from palaeontological evidence (Mikolaichuk et al., 1997). These data are also comparable with ages of 503–454 Ma from north of Lake Songkul by De Grave et al. (2011).

The Karadjorgo and Choloi Formations occur within the same belt and are lithologically similar. The difference is that the former contains more lava flows, whereas the latter is more tuffaceous. The Choloi suite was supposed to be younger than the Karadjorgo sequence (Middle Ordovician), based on preliminary fossil evidence, but many researchers considered them as possible analogs. Our dating of samples KG18, KG50b and KG63B indicate that the two formations are coeval and were apparently deposited within the same arc terrane.

A similar Early Ordovician age was obtained for dacitic tuff sample Mik 22 collected from the Karakorum Formation on the Tuyuk River in the Kungey Range. SHRIMP II dating of 4 idiomorphic, magmatic grains from this rock, presumed to be Neoproterozoic in age (Osmonbetov, 1980) yielded a mean $^{206}Pb/^{238}U$ age of 488.6 ± 2.1 Ma, whereas several slightly rounded, presumably detrital grains have ages of 833 ± 4, 860 ± 4 and 1123 ± 5 Ma (Table S4, Fig. S2f).

Essentially the same age was determined for sample Ki-2682 — a hornblende gneiss from the Burkhan River in the central Terskey Range that was previously correlated with the Mesoproterozoic Sarytor Complex (Kiselev et al., 1993). Numerous magmatic grains indicate that the protolith of the gneiss most likely was an igneous rock. SHRIMP II dating of 4 idiomorphic grains yielded a mean early Ordovician $^{206}Pb/^{238}U$ age of 493.5 ± 3.7, and one discordant grain has a latest Neoproterozoic minimum age of 685 ± 29 Ma (Table S4, Fig. S2d).

Sample KG73 is a fine-grained tuff–sandstone of unknown stratigraphic position that was collected on the southern slope of the Kyrgyz Range near Tyu-Ashuu Pass (Fig. 2), close to the entrance of the tunnel. The zircon grains are highly variable in their morphology and CL images, ranging from near-euhedral grains to well rounded oval to spherical varieties (Fig. S1j, inset). Forty-eight grains were analyzed and yielded three distinct age groups. The youngest and most distinct group defines a concordant cluster at about 465 Ma, and we interpret this to reflect arc-related magmatic activity in the Middle Ordovician. The second group of ages ranges from ca. 950 Ma to 1175 Ma and covers the time range generally known as Grenvillian. Such ages were reported by Kröner et al. (2013) from several basement terranes in the North Tianshan. The third age group ranges from ca. 1650–1900 Ma and reflects derivation of these grains from a late Palaeoproterozoic source.

Additionally, zircon grains from two sediments were analyzed by Kröner et al. (2007) from the Sulusai area on the SW slope of the Chu–Yili Mountains in southern Kazakhstan. These occur in the Djalair Naiman ophiolite belt that extends to the Trans-Yili Range in the

Please cite this article as: Rojas-Agramonte, Y., et al., Detrital and igneous zircon ages for supracrustal rocks of the Kyrgyz Tianshan and palaeogeographic implications, Gondwana Research (2013), http://dx.doi.org/10.1016/j.gr.2013.09.005

northern Tianshan (Avdeev and Kovalev, 1989; Kröner et al., 2007, and references therein). Sample KZ26 is a siltstone of the Cambrian Sulusai formation and KZ 23 is a turbidite sandstone of the latest Cambrian to Tremadocian Djambul Formation which rest on the lower Cambrian ophiolite. The youngest zircon in KG23 was dated at 489.6 ± 1 Ma and indicates derivation from an Early Ordovician arc source. Most grains in both samples are Palaeoproterozoic to Archaean, ranging in age from 2037 to 2782 Ma (see Kröner et al., 2007 for details and analytical data).

3.1.4. Magmatic rocks

Several magmatic rocks in the North Tianshan and adjacent southern Kazakhstan contain zircon xenocryst and old cores that carry a record of an older geological history. These were reported in Kröner et al. (2012, 2013, in press) and signify the existence of a Precambrian basement at depth. Numerous zircon grains with ages of 525, 828, 1637 Ma were found in monzodiorite sample Ki8287 from the western Terskey Range that yielded a Silurian emplacement age of 434.6 ± 4.8 Ma (Table S4, Fig. S2e), and ca. 1563 and 2001 Ma zircon xenocrysts occur in Mesoproterozoic granite sample KG70 on the Kökömeren River (Kröner et al., 2013, in press). In the Aktyuz area zircon xenocrysts were dated at 1180 Ma in a Neoproterozoic migmatite of the Kemin Complex (KG36) and at 783 Ma in an Early Ordovician granodiorite of the Dolpran pluton (KG37) (Kröner et al., 2012). Zircon grains in eclogites of the Makbal metamorphic complex in the western Kyrgyz Range have older cores with ages ranging from 665 to 1268 Ma, and one xenocryst from a Cambrian granodioritic gneiss in the same area yielded a Palaeoproterozoic age of 1443 Ma (Konopelko et al., 2012). In the Anrakhai area of southern Kazakhstan two xenocrysts with ages of 927 and 1214 Ma were dated in late Cambrian granodiorite sample P56/1 (Alexeiev et al., 2011). Finally, several zircon xenocrysts with ages ranging from 548 to 2288 Ma were found by Kröner et al. (2007) in an Early Ordovician arc-related granodiorite and a coeval metadacite from the Chiganak area southwest of Lake Balkhash.

3.2. The Middle Tianshan and Karatau–Talas terrane

The Middle Tianshan and Karatau–Talas terrane contain similar Neoproterozoic and early Palaeozoic sedimentary sequences with affinities to those in the Tarim basin but distinctly different from the North Tianshan. These sequences may be related to the Ishim–Middle Tianshan microcontinent (Windley et al., 2007). The samples from these terranes, include a) Neoproterozoic diamictites; b) Neoproterozoic and early Palaeozoic clastic deposits; c) Palaeozoic metamorphic rocks; d) Ordovician arc-related rocks, and e) Neoproterozoic granitoids.

3.2.1. Neoproterozoic diamictites

Neoproterozoic (Vendian in the Russian literature) diamictites were studied at two localities, namely west of Naryn and in the Chatkal area on the southern slope of the Talas Range. In both cases two samples were collected, one from the diamictite matrix and one from a large clast. Samples KG106 and KG107 are from the Shorashu Formation (Osmonbetov et al., 1982) and are exposed on the Karakysmak River draining the southern Talas Range (Table 1, Fig. 2). The section consists of green sandstone (KG107), siltstone, and shale with locally preserved grading and cross-bedding. It also includes turbidites with well defined Bouma sequences and massive interlayers of cobble conglomerate that contains rounded as well as angular granitoid clasts (sample KG106) and other lithologies, and these rocks were interpreted as diamictite (Mitrofanov, 1982; Korolev and Maksumova, 1984). The Shorashu Formation rests on the Beshtor granite (dated at 893 ± 3 Ma, Kröner et al., unpubl. data) with a basal conglomerate and changes up-section into shale and chert containing Cambrian and Lower Ordovician fossils (Osmonbetov et al., 1982). These relationships as well as correlation with the more precisely dated diamictite in the Naryn area (sample KG21) constrain the depositional age of the rocks as latest Neoproterozoic.

The zircon grains from granite clast KG106 are either near-spherical with typical metamorphic textures in CL images or have well rounded, oval shapes with oscillatory zoning. Only three grains were dated on SHRIMP II, and two of the apparently metamorphic grains have a mean $^{207}Pb/^{206}Pb$ age of 1804 ± 2 Ma, whereas the magmatic grain yielded an age of 1927 ± 20 Ma (Table S4, diagram not shown). All we can conclude from these data is that the clast was most probably derived from a Palaeoproterozoic source.

The zircon grains of sample KG107 have strongly variable morphologies, ranging from a few long-prismatic, near idiomorphic grains to well rounded and spherical-shaped varieties, and the CL images also reveal great diversity (Fig. S1q, inset). Thirty-six grains were dated (Table S1), and the data define two distinct and concordant to near-concordant groups. The younger group includes analyses continuously spread along Concordia between ca. 1800 and 1960 Ma and thus seems to characterize a distinct late Palaeoproterozoic source that is also reflected by one zircon in sample KG106, whereas the older group consists of individual analyses with ages from 2120 to 2880 Ma (Table S1, Fig. S1q) and may thus signify a different source. It would appear that the glacial material exclusively sampled Palaeoproterozoic to Archaean crust.

Sample KG21 represents the clastic matrix of a late Neoproterozoic diamictite of the Djetymtau Formation, exposed on the southern side of the Naryn River east of Naryn town. The glacial sequence is correlated with the Baykonur Formation of central Kazakhstan as well as with many other diamictite occurrences in Kazakhstan and Kyrgyzstan (Korolev and Maksumova, 1984; Chumakov, 2009). The rock contains variably sized clasts of mixed composition and up to 50 cm in diameter, and we analyzed zircon grains from an undeformed dacite clast reported below. The grains in sample KG21 are poorly to well rounded and highly variable in their CL images (Fig. S1c, inset), and the ages for 24 grains are concordant or near-concordant and range in age between 629 ± 8 and 2345 ± 20 Ma (Table S2, Fig. S1c). The youngest zircon age suggests that the diamictite formed during the global Marinoan glaciation (Shields, 2008), but Xu et al. (2009) determined an age of 615 ± 6 Ma for a volcanic bed interlayered with the Quruqtagh diamictites on the margin of the Tarim craton in NW China that, because of its similar age, may be equivalent to the Kyrgyz glacial rocks. Therefore, the glaciation in the Tianshan may be post-Marinoan (Xiao et al., 2004). Most detrital zircon ages in sample KG21 are in the range of 1750–2350 Ma and suggest a predominantly Palaeoproterozoic source for the diamictite matrix.

Nine zircons from dacite clast sample KG20, collected close to the matrix locality, were analyzed on SHRIMP II (Table S4). The zircon crystals are mostly euhedral and exhibit a fine to stripy oscillatory zoning, typical of felsic igneous rocks (Fig. S2a, inset). Five euhedral grains yielded a concordant $^{206}Pb/^{238}U$ age of 836 ± 4 Ma (Fig. S2a) that we interpret to reflect the time of felsic volcanism in the diamictite source area. One grain is concordant at 2340 ± 9 Ma and is a xenocryst (Fig. S1a) suggesting that the felsic volcanic rock may be a crustal melt from a Palaeoproterozoic source, similar to that reflected by the old detrital grains in the diamictite matrix. Surprisingly, three euhedral grains, morphologically indistinguishable from those of the 836 Ma generation, have a concordant mean age of 322 ± 3 Ma (Table S4, Fig. S2a) that is difficult to explain in view of the fact that the clast is undeformed, and the matrix only has a weak schistosity and reflects lower greenschist-facies metamorphism. There is no evidence for Carboniferous magmatism in the immediate area, but the age agrees with high-grade metamorphism in the suture zone separating the Middle and South Tianshan in Kyrgyzstan (Hegner et al., 2010). Also, Glorie et al. (2011) recorded early Permian magmatism in the same area and at other locations along the suture zone (Inylchek region), late Carboniferous ages were obtained by Glorie et al. (2011) and Konopelko et al. (2007, 2009). Therefore, we do not exclude the possibility that our 322 Ma zircon grains are of magmatic origin and have grown during

Please cite this article as: Rojas-Agramonte, Y., et al., Detrital and igneous zircon ages for supracrustal rocks of the Kyrgyz Tianshan and palaeogeographic implications, Gondwana Research (2013), http://dx.doi.org/10.1016/j.gr.2013.09.005

thermal overprinting. Our zircon separating technique involving panning makes it unlikely that the young grains are due to sample contamination.

3.2.2. Neoproterozoic and Palaeozoic clastic deposits

Neoproterozoic and Palaeozoic clastic deposits were studied in the Talas Range and in the Naryn area. Several samples were collected from thick sequences of slope turbidites of uncertain stratigraphic position (so-called Talas flysch), addressing the question about the provenance and stratigraphic age of this distinct unit.

Sample KG87 was collected from the northern slope of the Talas Range at the Kumyshtag River. These rocks were named, by different authors, either as Sarydjon Formation, presumably Neoproterozoic in age (Osmonbetov, 1980) or Tagyrtau Formation, provisionally assigned to the Cambrian and lower Ordovician (Tursungaziev and Petrov, 2008). Only 10 grains could be dated from this sample because of poor zircon yield, and the grains vary in shape between near-idiomorphic to well rounded and show good oscillatory zoning (Fig. S1m, inset). The concordant ages vary between 821 Ma for an almost euhedral grain and 2509 Ma for a well-rounded zircon (Table S1).

Two samples were collected on the Karabura River, on the northern side of Karabura Pass. Sample KG109 is a greenish sandstone, taken from a monotonous sequence of sandstone–siltstone–shale known as Uzunakhmat Formation, presumably late Proterozoic in age (Osmonbetov, 1980) (Table 1, Fig. 2). The zircon grains are extremely variable in their shapes and CL images, and near-idiomorphic as well as well rounded varieties occur, with most grains preserving good oscillatory zoning (Fig. S1r, inset). Forty-seven grains were analyzed (Table S1), and the concordant ages again exhibit two distinct groups. The younger group defines a near-unimodal distribution with an early Neoproterozoic age of ca. 860 Ma, whereas the older group consists of 7 grains with ages between ca. 1970 and 2770 Ma (Fig. S1r). These data seem to confirm a Neoproterozoic age of deposition <820 Ma and a predominantly early Neoproterozoic source with some input from an older terrane.

Sample KG110 is a brown, medium-grained sandstone of uncertain age that is assigned, by different authors, to either the Neoproterozoic Kyzylbel Formation (Osmonbetov, 1980) or the Late Ordovician Chukurchak Formation (Tursungaziev and Petrov, 2008); however, both ages are not proven. The grains are very similar to those in sample KG109, namely highly variable in morphology and CL images (Fig. S1s, inset). 48 grains were analyzed (Table S1), and the concordant data are remarkably similar to the age distribution in KG109. The dominant and unimodal group is represented by an age of ca. 820 Ma with three grains somewhat older at 950, 1120 and 1200 Ma, whereas the older group covers a large range between ca. 1800 and 2700 Ma (Fig. S1s). Judging from these ages, deposition in the Neoproterozoic seems indicated, but a younger age is not excluded, with a dominant source similar to that of KG109, and the older grains are derived from a Palaeoproterozoic to Archaean terrane.

Sample K 409 is a coarse-grained lithic sandstone with stratigraphic setting likely close to that of sample KG 110. According to different authors it relates to the Neoproterozoic Kyzylbel Formation (Osmonbetov, 1980), Late Ordovician Chukurchak Formation (Tursungaziev and Petrov, 2008), or early Paleozoic Postunbulak Formation (Voitenko and Khudoley, 2012). The thick sandstone unit, sampled for detrital zircon study, contains coarse-grained sandstone and small-pebble conglomerate interbeds pointing to a local provenance. The zircon crystals vary in shape between near-idiomorphic, long-prismatic grains and rounded, oval-shaped varieties. Most show well-preserved oscillatory zoning, but metamorphic grains and zircon grains with metamict interiors are also present. 24 grains were analyzed on SHRIMP II and provided concordant or near-concordant data with ages ranging from 559 ± 18 to 2995 ± 10 Ma (Table S5, Fig. S1u). Two zircon populations with ages of ca. 800–850 Ma and 1950–2500 Ma were identified. The younger population is represented by grains with well-preserved crystal shapes whereas older grains are typically well-rounded.

Sample K-412 is a lithic sandstone from the lowermost unit of the succession that is attributed to the Tagyrtau Formation and was provisionally considered to be Neoproterozoic (Osmonbetov, 1980; Voitenko and Khudoley, 2012), or Late Cambrian–Early Ordovician (Tursungaziev and Petrov, 2008) in age. The zircon morphology and age distribution are very similar to those in sample K-409. The zircon crystals vary in shape between near-idiomorphic, long-prismatic grains and rounded, oval-shaped varieties. Most show well-preserved oscillatory zoning, but metamorphic grains and zircons with metamict interiors are also present. 32 grains were analyzed on SHRIMP II, and the data define two clusters (ca. 750–1000 Ma and ca. 1950–2650 Ma) with the youngest age at 757 ± 23 and the oldest at 2644 ± 27 Ma (Table S5, Fig. S1v).

Khudoley and Semiletkin (2008) suggested on the basis of whole-rock Nd isotopic data for the above samples as well as their trace element patterns that the above zircon grains are derived from a large block including old continental upper crust. The most likely source, in our view, is the Ishim–Middle Tianshan microcontinent that extends from the Tianshan to the western part of northern Kazakhstan (Avdeev and Kovalev, 1989; Windley et al., 2007; Kröner et al., 2013) and whose southern part is shown in Fig. 1.

Meert et al. (2011) dated igneous and detrital grains from Neoproterozoic tuff and tuff–sandstone of the Kurgan Formation in the northern part of the Karatau–Talas terrane, within the Lesser Karatau Range of southern Kazakhstan. They obtained Concordia ages of 766 ± 7 and 831 ± 15 Ma for idiomorphic zircon grains from two tuff horizons, whereas tuff–sandstone yielded detrital grains ranging in age from 2032 to 2816 Ma which these authors interpreted to be derived from Lesser Karatau basement rocks. However, the oldest exposed basement in this area is Meso-(?) and Neoproterozoic in age (Abdulin et al., 1986), and other source areas should therefore be considered.

Sample KG19 is a sandstone of the Ichkebash Formation, collected in the Naryn area from the southern slope of the Moldotau Range (Table 1, Fig. 2). These rocks contain Upper Ordovician trilobites and graptolites (mainly Sandbian and Katian stages, Neievin et al., 2011). The zircon population is highly variable in morphology with most grains distinctly rounded and some even spherical in shape. Likewise, the CL images are highly variable, and some grains display good oscillatory zoning whereas others show complicated patterns including partial recrystallization and partial metamictization (Fig. S1b, inset). Twenty-four zircon grains were analyzed and provided concordant ages ranging between 758 and 2355 Ma (Table 2, Fig. S1b). This age range is also reflected by gneissic rocks in the Kyrgyz Tianshan (Kiselev and Korolev, 1972; Kiselev et al., 1993; Kiselev, 1999; Kröner et al., 2012, 2013), and it is therefore most likely that the sandstone was derived from a Precambrian source of the Ishim–Middle Tianshan microcontinent.

3.2.3. Palaeozoic metamorphic complexes

Palaeozoic metamorphic complexes in the Middle Tianshan occur west of Naryn, south of Toktogul, in the South Chatkal Range, and also within a narrow block at the base of the northern slope of the Atbashi Range, north of the Atbashi–Inylchek fault (Bakirov, 1978; Fig. 2).

Only 12 detrital grains could be analyzed from sample KG93, a sillimanite-bearing paragneiss collected from a sequence of isoclinally folded and high-grade metasediments of the Takhtalyk Complex (Bakirov, 1978) on the eastern bank of the Karasu River and the northern side of the Talas–Ferghana Fault south of the Toktogul Reservoir (Table 1, Fig. 2). These rocks were previously considered to be early Precambrian in age (Bakirov et al., 2003). The zircon crystals are mainly well rounded with many oval to spherical shapes, but long-prismatic grains with some rounding at their terminations also occur. The CL images are highly variable, and some reveal core–rim relationships (Fig. S1n, inset). All this suggests a fairly heterogeneous source. Although 12 grains are not representative of the entire sample, the relatively narrow spread in ages between ca. 695 and 750 Ma (Table S2,

Please cite this article as: Rojas-Agramonte, Y., et al., Detrital and igneous zircon ages for supracrustal rocks of the Kyrgyz Tianshan and palaeogeographic implications, Gondwana Research (2013), http://dx.doi.org/10.1016/j.gr.2013.09.005

Fig. S1n) for the youngest group suggests this rock not to be older than late Neoproterozoic. An older group provided partly discordant Palaeoproterozoic ages between ca. 1860 and 1900 Ma.

A sample of a medium-grade metasediment was described by Glorie et al. (2011) from the northern slope of the Atbashi Range, north of the Atbashe–Inylchek fault i.e. from the Kembel metamorphic complex of the Middle Tianshan according to the regional geological map (Tursungaziev and Petrov, 2008). Several detrital grains were dated at ca. 788, 1004, and 1174, and several older grains are discordant and may be as old as 2441 Ma (Glorie et al., 2011).

3.2.4. Ordovician arc-related sequences

Ordovician arc-related sequences are uncommon in the Middle Tianshan and only locally occur in the South Chatkal Range within the Semizsai Complex that was previously thought to be Palaeoproterozoic in age (Bakirov et al., 2003 and references therein). Sample KG97 is a volcanic-derived chlorite–albite schist, exposed in a sequence of strongly folded and lineated felsic to intermediate tuffaceous rocks of the Semizsay metamorphic Complex, and was collected on the Kasansay River on the South Chatkal Range (Table 1, Fig. 2). The zircon crystals are mostly long-prismatic, euhedral and occasionally with slightly rounded terminations, and the CL images reveal well-preserved and simple magmatic growth textures (Fig. S1o, inset). Thirty-six zircon grains were analyzed (Table S1) and, as in the previous cases, these provided well-grouped data that yielded a mean Concordia age of 460.6 ± 1.4 Ma (Fig. S1o) and most likely reflects arc volcanic activity in the southwestern Middle Tianshan at the end of the Middle Ordovician. De Grave et al. (2012) also reported evidence for late Cambrian to Late Ordovician magmatic activity north of the Nikolaev Line around Lake Song-Kul.

Sample KG104 is a strongly foliated biotite–muscovite–feldspar schist of the Semizsay metamorphic complex of the Middle Tianshan. It was collected on the Ishtamberdy River in the South Chatkal Range area (Table 1, Fig. 2) and shows a similar age pattern as sample KG97. The zircon crystals are variable in their morphology, and many are long-prismatic with some distinct rounding at their terminations, whereas others are oval-shaped. The CL images are also highly variable, indicating great diversity in the zircon population (Fig. S1p, inset). 48 grains were analyzed (Table S1), are mostly concordant, and define four age groups. The youngest group represents an age cluster at about 460 Ma, most likely reflecting latest Middle Ordovician arc magmatism, with one grain at ca. 510 Ma possibly sampling an earlier volcanic event (Table S1). The second group is only defined by four grains with Grenville-type ages of ca. 1000–1200 Ma, whereas the third group ranges from ca. 1430 to 1850 Ma. The oldest group consists of 3 grains with ages of ca. 2590, 2800 and 3000 Ma (Fig. S1p). It is obvious that the Precambrian detrital grains reflect a very heterogeneous Mesoproterozoic to Archaean source region for this metasediment, and combination of the well-grouped near-idiomorphic Palaeozoic zircon grains with the well-rounded Precambrian grains suggests a continental margin arc setting as the most likely scenario for this rock.

3.2.5. Granitoid rocks

Granitoid rocks with zircon xenocrysts and inherited cores were documented from the Middle Tianshan at several sites by Glorie et al. (2011) and Seltmann et al. (2011). Two samples of Neoproterozoic granite and felsic volcanic rocks from the Akshiyryak and Djytymbel Ranges contain late Neoproterozoic to Palaeoproterozoic grains dated by ICPMS between 831 and 2324 Ma (Glorie et al., 2011). One inherited zircon core dated at 998 Ma was also reported in a sample from the 303 Ma Ulan granite from the southern part of the Middle Tianshan (Seltmann et al., 2011).

3.3. South Tianshan

Samples KG27 and 29 are paragneisses from the Atbashi Metamorphic Complex, a subduction–accretion terrane that occurs on the northern margin of the South Tianshan (Biske, 1996) and contains lenses of eclogite dated at 319 ± 4 Ma (Hegner et al., 2010). The tectonically dismembered sedimentary assemblage consists of garnet–muscovite schist, garnet–albite–muscovite–chlorite–(amphibole) schist, mica schist, phyllite, and minor lenses of marble and metavolcanic rocks, and the grade of metamorphism in these strongly deformed rocks varies from greenschist- to blueschist-facies (Bakirov, 1978; Bakirov and Kotov, 1988). The depositional age of low-grade schists is Silurian to Early Devonian, based on Tabulata corals in carbonate lenses (Biske et al., 1985), whereas the higher-grade metasediments are either inferred to be Proterozoic (Bakirov et al., 1974; Tursungaziev and Petrov, 2008) or middle Palaeozoic (Osmonbetov, 1980). Hegner et al. (2010) dated 24 detrital grains from a metagreywacke associated with eclogite in the northern Atbashi Range (KG25) and obtained ages ranging from 427 to ca. 2500 Ma, which they suggested were mainly derived from the Tarim craton. We have analyzed 24 additional detrital grains from the same sample, and these are mostly well rounded with oscillatory-zoned CL images. The ages vary between 442 ± 14 and 2645 ± 29 Ma (Table S2, Fig. S1d), with only a few early Palaeoproterozoic to Archaean grains, and are in the same range as found by Hegner et al. (2010).

Sample KG27 is a compositionally layered paragneiss of clastic derivation from the Aktala area, close to where the sample of Hegner et al. (2010) was collected (Fig. 2). Only 12 zircon grains were dated by ICPMS in Mainz from this sample which are variably rounded and oscillatory-zoned (Fig. S1e inset), and the ages range from 410 ± 5 to 932 ± 11 Ma (Table S2, Fig. S1e). The youngest age confirms the Early Devonian assessment of Khristov and Mikolaichuk (1983), whereas the older ages are similar to those obtained by Hegner et al. (2010). Sample KG29 is a fine-grained quartzo-feldspathic paragneiss collected at Tashrabat (Table 1, Fig. 2) where the metamorphic grade is generally lower than at Atbashi. The zircon crystals are again variably rounded, and most exhibit oscillatory zoning with some grains showing core–rim relationships and metamictization (Fig. S1f, inset). Twenty-five grains were analyzed, and the range of ages is significantly greater than that of KG2, possibly due to the larger number of analyses. Six round grains with typical CL-features of metamorphic grains such as light gray images (low-U) and broad or no zonation have $^{206}Pb/^{238}U$ ages of 329 ± 5 to 336 ± 6 Ma and may reflect Carboniferous metamorphism. However, they also match early Carboniferous magmatic zircon ages from intrusive rocks associated with the South Tianshan suture (Glorie et al., 2011). The two youngest detrital grains with ages of 418 ± 6 and 424 ± 6 Ma are in line with the depositional age estimate of Biske et al. (1985), whereas the oldest grain at 2620 ± 27 Ma is in the same range as the metagreywacke dated by Hegner et al. (2010).

The occurrence of numerous grains with ages around 440–450 Ma in samples KG25, 27 and 29 as well as the greywacke sample dated by Hegner et al. (2010) indicates a provenance in the North Tianshan where granite batholiths with such ages are widespread. The North Tianshan, similar to the Chinese Central Tianshan, may represent a fragment of Tarim derived by spreading in the late Precambrian (e.g., Jian et al., 2013; Lei et al., 2013), and this explains why Precambrian ages are similar in the two terranes. This aspect is further discussed below.

Finally, we dated detrital grains from a sample of garnet micaschist (Ki2236) of the Choloktor Complex (Mikolaichuk and Buchroithner, 2008), exposed on the main watershed of the South Tianshan in the Kokshaal Range south of the Sarydjaz River (Table 1, Fig. 2). This location is close to the Kyrgyz–Chinese border, and there is little doubt that this sample belongs to the Tarim basement, tectonically wedged between Palaeozoic rocks. The zircon morphology is strongly variable between rare near-idiomorphic and abundant well rounded to near-spherical grains with equally variable CL images including oscillatory-zoned as well as obvious metamorphic grains (Fig. S1w, inset). 60 grains were analyzed, and although there are several concordant results, many grains yielded slightly to significantly discordant data (Table S1). As in several previous samples, the age range is exceptionally large between ca. 600 and 3450 Ma (Fig. S1w). There are a few Neoproterozoic ages

Please cite this article as: Rojas-Agramonte, Y., et al., Detrital and igneous zircon ages for supracrustal rocks of the Kyrgyz Tianshan and palaeogeographic implications, Gondwana Research (2013), http://dx.doi.org/10.1016/j.gr.2013.09.005

at about 600, 800 and just over 900 Ma and many Mesoproterozoic grains with ages between 1000 and ca.1340 Ma, and the most dominant population is at ca. 2500 Ma with many of these grains displaying variable discordance. A few grains have ages between 2600 and 3420 Ma (Inset in Fig. 4b, Table 2, Fig. S1w). The similarity of this age pattern with known age distributions in the Tarim craton (see below and Rojas-Agramonte et al., 2011) is obvious, but the more important implication is that this pattern is similar to those for detrital grains from several metasediments in the North and Middle Tianshan, making their derivation from a Tarim source very likely. This aspect is further discussed below.

4. Hf-in-zircon isotopes for selected samples from the Kyrgyz Tianshan

We have analyzed a few grains of the Kyrgyz Tianshan detrital zircon populations for Hf isotopes in order to assess their crustal history. Previous studies have shown that many igneous rocks in the Kyrgyz North and Middle Tianshan represent crustal melts, based on their Nd whole-rock and Hf-in-zircon isotopes (Kröner et al., 2012, 2013, in press), and this supports the conclusion that there is more Precambrian basement at depth than is obvious from surface outcrops and that there was relatively little crustal growth during the accretionary history of the belt (Kröner et al., in press). Many of the early Palaeozoic granitoid intrusions exposed in the Kyrgyz North Tianshan are most likely derived from melting of ca. 1.1 Ga protoliths (Kröner et al., 2013), suggesting that this Mesoproterozoic basement is extensive.

The following data are from a reconnaissance study, and the analytical procedure is described in the Appendix A. The data are shown in Table S6, and the individual data are plotted in Hf evolution diagrams shown in Fig. S3. A summary diagram is presented in Fig. 3 below. Sample KG50b is an arc-derived tuff–sandstone with the zircon grains forming a coherent group defining an age of 493 Ma that we interpreted as the time of arc magmatism. The Hf isotopic data for 5 grains from this sample all have positive $\varepsilon_{Hf(t)}$-values (Table S6, Fig. S3a), suggesting that the host rock formed from a juvenile source. This is one of the rare cases in the Tianshan where the host rock of the zircon grains probably represents an intra-oceanic arc complex. A similar case is provided by sample KG118, a cherty siltstone from the East Terskey Range with zircon ages between ca. 1000 and 2800 Ma (Table S1, Fig. S1t). Three grains with ages around 1500 Ma were analyzed for their Hf isotopic ratios and yielded positive $\varepsilon_{Hf(t)}$-values (Table S6, Fig. S3g), suggesting that these grains were derived from a short-lived late Palaeoproterozoic crustal source.

Zircon grains from all other samples analyzed for Hf isotopes either provided predominantly negative $\varepsilon_{Hf(t)}$-values or mixed results with data varying between negative and slightly positive $\varepsilon_{Hf(t)}$-values (Table S6, Fig. S3). These show that many sedimentary rocks in the North Tianshan have diverse sources, including rocks with a long crustal history and minor volumes with short crustal residence times, i.e. rocks either derived from magmatic underplating or subduction-related arc magmatism. A particular interesting sample is KG76, a quartzite from the South Kyrgyz Range, NW of Talas, where the detrital zircon ages range from 1730 to 3780 Ma (Table S1, Fig. S1l). The $\varepsilon_{Hf(t)}$-values are predominantly negative with some values in the slightly positive field (Table S6, Fig. S3c), but there is no clear evidence of a primitive source for these grains. The oldest zircon of 3780 Ma has a Hf crustal model age of just over 4 Ga, and although this is not a reliable age constraint in view of the uncertain $^{176}Lu/^{177}Hf$ crustal ratio at this time, it underlines the antiquity of the source area of this quartzite.

The composite Hf evolution diagram of Fig. 3 displays the great diversity and heterogeneity of detrital zircon sources shown by the Tianshan metasediments and confirms previous suggestions that much of the Kyrgyz North Tianshan consists of reworked crustal material, some of it with a long history possibly dating back to the Hadean, whereas juvenile crustal sources are less prominent but seem to have contributed to crustal growth since the Archaean.

5. Comparative Precambrian zircon age pattern for the Tianshan and Tarim craton

In the following sections and accompanying diagrams we first compare and contrast the age patterns derived from the Kyrgyz/Kazakh detrital and xenocrystic Precambrian zircon ages for the North, Middle and South Tianshan. We then compare these patterns with data from the Chinese Central Tianshan (including Yili Block) and the Tarim craton. In this comparison we exclude arc-related early Palaeozoic zircon ages because these are clearly reflecting the accretionary history of the Tianshan and are thus of relatively local provenance. Most authors agree that the Kyrgyz North and Chinese Central Tianshan constituted an arc terrane in the Ordovician–Silurian (Mikolaichuk et al., 1997; Charvet et al., 2007; Degtyarev et al., 2012; Kröner et al., 2012; De Grave et al., 2013).

The available data were compiled in Excel spreadsheets (Tables S7–S9) from which probability distribution diagrams were constructed. These provide an informative presentation of multiple age populations as well as information about the precision of measurement that is lost in histograms. Zircon ages were compiled using $^{206}Pb/^{238}U$ data for ages <1000 Ma and $^{207}Pb/^{206}Pb$ data for ages >1000 Ma as explained in Section 3. Data from the literature with more than 30% discordance or uncertainties >60 Ma were not considered in our compilations. The diagrams are subdivided into two parts, one showing the age patterns between 500 and 1800 Ma (Fig. 4a), the other showing the patterns between 1500 and 4000 Ma (Fig. 4b). Of necessity, this compilation is somewhat unbalanced because igneous emplacement ages are reported as one figure although several zircon grains were analyzed, whereas for detrital populations each grain-age is listed separately. Therefore, the detrital ages receive more weight than the magmatic emplacement or mean metamorphic ages.

5.1. Comparative age pattern for the Kyrgyz North, Middle and South Tianshan

Our compilation includes 325 ages for the North Tianshan, 640 ages for the Middle Tianshan, and 128 ages for the South Tianshan (Fig. 4, Table S7). The North Tianshan age frequency distribution shows several small peaks between ca. 700 and 1100 Ma (Fig. 4a), reflecting both detrital zircon ages from metasediments presented in this paper and granitoid gneisses dated in Kröner et al. (2012, 2013, in press). Similarly, the Middle Tianshan shows small peaks between 700 and 950 Ma and a major peak at ca. 820 Ma that reflects two sedimentary samples from the Lesser Karatau Range in southern Kazakhstan. Zircon ages around 800 Ma may reflect a magmatic event preserved in tuffs and may therefore reflect a local provenance. For example, a mean age of 818 ± 10 Ma was obtained for magmatic zircon grains in a tuff sample from the Kurgan Formation in the Karatau–Talas zone (Kröner, Rojas-Agramonte, Alexeiev, unpubl. data). Idiomorphic grains with ages around 800 Ma in our samples K-409 and K-412 may also indicate a local volcanic provenance. There are also many magmatic rocks with the ages of ca 800 Ma in southern Kazakhstan as well as the North and Middle Tianshan, including tuffs (Meert et al., 2011) and rhyolites (Kröner et al., 2007). Granitoid gneisses of this age are exposed in the Aktyuz area of the Kyrgyz North Tianshan (Kröner et al., 2012). All these rocks are likely sources for detrital grains because they occur in the same area. However, we cannot exclude the possibility that these Neoproterozoic to late Mesoproterozoic zircon grains are derived from sources outside the Tianshan such as the Tarim craton that shows a similar age pattern.

A major peak at about 1170 Ma in Fig. 4a reflects Grenville-age terranes and associated metasediments in the North Tianshan that were discussed in Kröner et al. (2013, in press). There is no comparable peak in either the Middle Tianshan or in any of the other possible source

Please cite this article as: Rojas-Agramonte, Y., et al., Detrital and igneous zircon ages for supracrustal rocks of the Kyrgyz Tianshan and palaeogeographic implications, Gondwana Research (2013), http://dx.doi.org/10.1016/j.gr.2013.09.005

terrains considered here, including the Tarim craton. This aspect is further discussed in Section 5.3. Minor peaks at ca. 1380, 1480 and between 1530 and 1610 Ma in both the North Tianshan and Middle Tianshan are difficult to explain since they reflect a period of generally little magmatic activity worldwide (Condie and Aster, 2010). A major feature of the North Tianshan age pattern is a distinct and sharp peak at ca. 1890 Ma (Fig. 4b), reflecting zircon grains from samples KG76 and KG118. This broad peak is also evident in the Middle Tianshan age pattern (Fig. 4b). A further sharp peak at ca. 2500 Ma in the South Tianshan corresponds to two late Palaeoproterozoic to late Neoarchaean peaks in the North Tianshan and also matches a peak in the Tarim craton. In contrast, supracrustal rocks with a Neoarchaean source are not evident in the Middle Tianshan. The extremely old ages of 3810 ± 28 and 3475 ± 12 Ma found in samples KG76 (western North Tianshan) and Ki-2236 (South Tianshan) are exotic and are not matched by any data from the other terranes (Fig. 4b). However, a zircon xenocryst age of 3888 ± 1.5 Ma, reported by Kröner et al. (2008) from a Silurian pluton in northern Kazakhstan, east of Kokchetav, may support a possible link between the Tianshan and the Kokchetav block, in addition to similarities in 1050–1150 Ma ages (Kröner et al., 2013, in press).

5.2. Comparative age patterns for the Kyrgyz and Chinese Tianshan

From the evidence of magmatic zircon ages for some granitoid gneisses as well as xenocrystic grains and whole-rock Nd isotope data most authors agree that the Chinese Central Tianshan and Yili Block consist of a Precambrian basement (e.g., Ma et al., 2012b; Jian et al., 2013; Lei et al., 2013; Ma et al., in press). Recent comparative data for the Tianshan and Tarim craton suggest that the two were part of one continental block, at least until the end of the Precambrian (Luo, 1989; Lei et al., 2011; Ma et al., 2012a,b). There are also similarities in some lithostratigraphic sequences supporting such connection (Shu et al., 2011; Zhu et al., 2011a,b; Lei et al., 2012). However, these similarities do not necessarily mean that the Central Tianshan was rifted off the Tarim craton as a coherent block, as is shown in many published cartoons (e.g., Gao et al., 2009; Charvet et al., 2011). Our previous work in the Kyrgyz Tianshan suggests that Precambrian terranes are tectonically wedged between Palaeozoic arc-derived assemblages, and this may not imply a continuous Precambrian basement but several distinct microcontinental fragments (Kröner et al., 2012, 2013, in press), similar to the situation in Mongolia (e.g., Kozakov et al., 2007; Demoux et al., 2009). Furthermore, geological maps of the Chinese Central Tianshan (Li and Xu, 2007) show numerous blocks of little studied ultramafic rocks, and at least some of these may have an ophiolitic origin and may represent possible continuations of the early Palaeozoic Kyrgyz–Terskey, Djalair–Naiman or Erementau–Yili suture zones (Windley et al., 2007 and references therein). The latter are well documented in southern Kazakhstan and Kyrgyzstan but were not identified so far in the Chinese Tianshan. Therefore, the Chinese Central Tianshan may also consist of several distinct Precambrian continental blocks, tectonically wedged between Palaeozoic terranes. At present, the Central Tianshan is a relatively narrow domain bounded by sutures in the north and south and consisting predominantly of Precambrian crystalline rocks infolded with minor early Palaeozoic volcano-sedimentary successions and granitoid intrusions (Liu et al., 2004; Shu et al., 2004).

Ma et al. (2012b, in press) summarized the available emplacement and xenocryst ages for Central Tianshan granitoid rocks that range between 340 and 1750 Ma, and Ma et al. (2013) reported detrital igneous zircon ages from Precambrian metasediments going back to 2544 Ma. Hf-in-zircon isotopic data on Palaeozoic granitoids of the Central Tianshan show most of these rocks to be derived from Meso-to Palaeoproterozoic crust, but some granitoids also show input from mantle-derived sources (Ma et al., in press). The published zircon ages for the Central Tianshan are not, however, representative of the entire belt and mostly concentrate on rocks exposed in the relatively small Balunai area SW of Urumqi (Ma et al., 2012a,b, 2013).

Fig. 4 (second from top) shows published Precambrian igneous and detrital zircon ages for the Chinese Central Tianshan, compiled from data reported in Ma et al. (2012a,b) and other sources (see Table S2). The age pattern for the Neoproterozoic is very similar to that of the Kyrgyz Tianshan (Fig. 4, bottom) in showing several peaks between ca. 700 and 850 Ma, and a major peak at ca. 960 Ma corresponds to smaller peaks in the Kyrgyz North and Middle Tianshan whereas in the Kyrgyz South Tianshan this peak is broad between ca. 920 and 1050 Ma. Small peaks between 1110 and 1280 Ma correspond to similar data in the Kyrgyz Tianshan but are not as prominent as in the Kyrgyz North Tianshan.

The Palaeoproterozoic to Archaean age pattern (Fig. 4b) shows a major peak at ca. 1800 Ma in the Chinese Central Tianshan, matched by similar peaks, although at slightly different times, in the Kyrgyz Tianshan. Another significant peak at 2160 Ma is only matched by much smaller peaks in the Kyrgyz Middle Tianshan and South Tianshan. No major peak at about 2500 Ma is apparent in the Chinese Tianshan. Thus, although the age patterns between the Chinese and Kyrgyz Tianshan correspond broadly there are also significant differences. This may partly be due to the fact that the data distribution in the Chinese Tianshan does not cover the entire terrane.

5.3. Composite Precambrian zircon age patterns for the Tianshan and Tarim craton

The Precambrian evolution of the Tarim craton has recently been reviewed by Zhang et al. (2013) who also presented a compilation of isotopic ages based on references up to 2011. Further data on Palaeoproterozoic rocks from the northeastern margin of the craton were presented by He et al. (in press) and Wang et al. (in press), whereas Xu et al. (2013) reported detrital zircon ages from sediments recovered from deep drilling in the Tarim basin. These zircon ages have been combined with the compilation presented in Rojas-Agramonte et al. (2011) and are presented in the relative probability plot of Fig. 4 (top) that includes 2073 zircon ages from Tarim. These may, however, not be truly representative of the craton whose Precambrian rocks are only exposed along the northeastern, southwestern and southeastern craton margin whereas its center is covered by Palaeozoic to Cenozoic sediments (e.g., He et al., in press). The oldest published zircon ages for the Tarim basement are 3674 ± 56 and 3665 ± 15 Ma for inherited zircon cores (Li et al., 2001; Lu et al., 2008), and these data suggest the presence of early Archaean crust in the Altyn Tagh Uplift of the southeastern Tarim craton (Ge et al., 2013). More evidence for an early Archaean crustal component was presented by Ge et al. (2013) from a Hf-in-zircon isotope study of migmatites exposed near the city of Korla on the northern margin of the craton. These authors reported Hf crustal model ages between 3.3 and 3.8 Ga from ca. 2.3 Ga old zircon in a ca. 1.85 Ga stromatic migmatite, and these are remarkably close to the Hf model ages calculated for our samples KG76 and Ki-2236 (see Table S6, Fig. 3).

A small but broad peak at 2300–2500 in Tarim is also apparent in the Chinese Tianshan, whereas a peak at 2150 Ma in the Chinese Tianshan does not have a counterpart in Tarim. This is most likely due to insufficient sampling in the Chinese Tianshan and limited exposures of Precambrian rocks in Tarim.

A major magmatic and metamorphic event occurred between 2.0 and 1.8 Ga and is interpreted by most authors to have led to crustal stabilization and formation of a Tarim cratonic nucleus (Zhang et al., 2013), and speculations abound that this may have been related to Columbia supercontinent aggregation in the late Palaeoproterozoic (Zhang et al., 2013). This event is reflected by a major peak in Fig. 4 that is also apparent in all the Tianshan terranes.

Zircon ages between ca. 1600 and 1400 Ma were found in all Tianshan terranes and are also present in the Tarim age pattern (Fig. 4). These ages are difficult to interpret because no igneous or metamorphic event is known for this time period in any of the other cratons

Please cite this article as: Rojas-Agramonte, Y., et al., Detrital and igneous zircon ages for supracrustal rocks of the Kyrgyz Tianshan and palaeogeographic implications, Gondwana Research (2013), http://dx.doi.org/10.1016/j.gr.2013.09.005

bordering the CAOB or from basement terranes within the belt. The period also has rather few zircon ages worldwide in a global compilation of ca. 200,000 detrital zircon ages (Voice et al., 2012). Therefore, the origin of these grains in the Tianshan and Tarim remains unexplained.

A further event at about 1050–900 Ma, locally known as Tarimian orogeny and including calc-alkaline arc-type volcanism, is well documented by zircon ages, but its tectonic significance is uncertain (Lu et al., 2008). Zhang et al. (2013) and several other Chinese authors speculated that this phase of igneous–metamorphic activity was related to the assembly of the Rodinia supercontinent, but there are no palaeomagnetic data to substantiate this assumption.

Ca. 780–735 Ma bimodal volcanic rocks and minor 650–635 Ma mafic dykes along the northern margin of the Tarim craton are generally interpreted to signify a rifting event possibly related to break-up of Rodinia (Zhu et al., 2008, 2011a,b; Zhang et al., 2013) and perhaps triggered by a plume (Long et al., 2011). OIB gabbro and basalts of the Dalubayi ophiolite massif in the western Nalati Range of the Chinese Central Tianshan yielded late Neoproterozoic zircon ages of 600 ± 15 and 590 ± 11 Ma (Yang et al., 2005), which imply that some oceanic crust may already have existed between Tarim and the Central Tianshan since latest Precambrian time. Whatever the cause, fragments of the Tarim craton have been interpreted to occur within the Palaeozoic terranes of the Central Asian Orogenic Belt in Mongolia and Kyrgyzstan, mainly on account of the presence of ca. 1100–900 Ma rocks (e.g., Demoux et al., 2009; Rojas-Agramonte et al., 2011; Kröner et al., 2013).

The Tarim break-up process may have continued into the early Palaeozoic, and Charvet et al. (2007) suggested that the Chinese Central Tianshan began to separate from the Tarim craton in the Ordovician–Silurian due to formation of a rift, developing into a back-arc basin, as a result of southward subduction of the Central Tianshan Ocean. Jian et al. (2013) argued that this rifting process continued into the early Carboniferous.

Much of the above Tarim evolution is reflected in the zircon record as shown in Fig. 4 (top), and there is remarkable agreement between the age pattern for the Tarim craton and Precambrian detrital as well as igneous grains from the Kyrgyz and Chinese Tianshan. The Tarim peak at about 920 Ma has a long "tail" up to about 1100 Ma so that many of the Grenvillian ages do not stand out because of the large number of analyses incorporated in this frequency probability plot. However, the range of Tarim ages between ca. 900 and 1100 Ma is also reflected in the Chinese Central Tianshan as well as the Kyrgyz North and South Tianshan. This is less evident in the Middle Tianshan where a strong peak at about 830 Ma certainly reflects a Neoproterozoic source area that is also seen in all the other terranes discussed here. This may reiterate the concept of the Middle Tianshan representing a distinct tectonic domain receiving detritus from a different source as the North Tianshan. The Tarimian orogeny, as defined by Lu et al. (2008) is based on relatively few ages from a restricted domain within Tarim, and the age range 900–1050 Ma may therefore not be representative of this event, considering that the entire Grenvillian orogeny on North America consisted of four distinct phases covering an age range of 250 Ma from about 1450 to 900 Ma (Hynes and Rivers, 2010).

In summary, we reiterate our previous conclusions that much of the detrital zircon populations in metasediments of the Tianshan were either derived from the craton itself or from cratonic fragments already rifted off in the Neoproterozoic and then becoming incorporated into the Central Asian accretionary collage.

6. Significance of detrital zircon ages for CAOB palaeogeography and tectonics

Mossakovsky et al. (1993) and Dobretsov and Buslov (2007) argued that most Precambrian continental fragments within the CAOB are derived from the North Gondwana margin without being specific on location. Rojas-Agramonte et al. (2011) discussed this issue in their compilation of detrital and xenocrystic zircon ages from Mongolia and argued for a Tarim origin because there are no major Grenville-age terranes on the northern Gondwana margin except for Venezuela and Colombia. The question, therefore, is whether Tarim was part of northern Gondwana or constituted a separate, independent continent. Li et al. (1996) suggested a Tarim–northwest Australia connection in the late Neoproterozoic on the basis of scanty palaeomagnetic and geological data, and Zhan et al. (2007) reiterated this on the basis of a palaeopole for ca. 595 Ma mixtite-bearing metasediments and metavolcanic rocks from the Aksu area and placed Tarim north of Australia near the Kimberley region. The main arguments for the Kimberley–Tarim connection are that the ages of mafic dykes of 798–811 Ma in the Kimberley are not statistically different from those of the Aksu area at 785 ± 31 Ma (Zhan et al., 2007). In addition, the Neoproterozoic Sturtian tillites and overlying sedimentary succession in the Kimberley are comparable to those of the Tarim basin (Brookfield, 1994, and references therein). The main problem with this model is that there is no evidence for a Grenvillian-age event in northern Australia, whereas such rocks are abundant in Tarim as shown above and in Rojas-Agramonte et al. (2011).

Huang et al. (2005) proposed a different scenario in which the Tarim Block rifted off Western Australia during the break-up of the Rodinia supercontinent at about 820–750 Ma. This model is also adopted on the Rodinia map (Li et al., 2008), but Li et al. (2013) have now revised the relative position slightly by having the southern margin of Tarim connected to Australia rather than the originally proposed northern margin. Some possible geological support for this comes from the occurrence of ca. 1100 Ma old rocks of the Northampton Complex, an elongate Grenville-age block situated north of Geraldton and belonging to the Mesoproterozoic Pinjarra Orogen (Ksienszyk et al., 2012, and references therein).

7. Conclusions

Our Precambrian zircon ages for the Kyrgyz Tianshan and a comparison with published data from the Chinese Tianshan and the Tarim craton support the concept that the source terrane for many Tianshan sediments is the Tarim craton or Precambrian crustal blocks that were rifted off Tarim in the late Neoproterozoic and now constitute basement terranes within the Tianshan orogen. A similar conclusion has previously been reached by Rojas-Agramonte et al. (2011) from zircon age patterns in Mongolia and is mainly based on the widespread occurrence of Grenville-age zircon grains. Although reliable Neoproterozoic to early Palaeozoic palaeomagnetic data for Tarim are not available, its most likely palaeogeographic position was somewhere near the northwestern margin of Australia (Li et al., 2013). A scenario involving fragmentation of Tarim and perhaps other Precambrian fragments originating from northeastern Gondwana during the early evolution of the CAOB is therefore likely, considering the similarity in basement geology between these blocks and Tarim. Thus, we envisage an archipelago-type scenario for the Palaeo-Asian Ocean south of the Siberian craton in the late Neoproterozoic to early Palaeozoic in which numerous island arcs and Precambrian crustal fragments drifted northwards (in present coordinates) and were amalgamated and tectonically stacked together during several ocean closure and accretion–collision events. Such a scenario is surprisingly similar to what has been envisaged for the evolution of Indonesia in the Mesozoic and Cenozoic where Hall and Sevastjanova (2012) have shown that Mesozoic rifting of fragments from the Australian margin, followed by Cretaceous collisions and Cenozoic collision of Australia with the SE Asian margin, thus creating arc terranes, often floored by Australia-derived older crust. We follow Hall and Sevastjanova (2012) in emphasizing that in both Central Asia and Indonesia continental crust has arrived in the region in multiple episodes and has been fragmented and juxtaposed by subduction-related processes. Continental growth during this process was minimal (Kröner et al., in press).

Our zircon data also support the conclusion of several Chinese authors that the Central Tianshan and, by implication, much of the Kyrgyz

Please cite this article as: Rojas-Agramonte, Y., et al., Detrital and igneous zircon ages for supracrustal rocks of the Kyrgyz Tianshan and palaeogeographic implications, Gondwana Research (2013), http://dx.doi.org/10.1016/j.gr.2013.09.005

North and Middle Tianshan are underlain by Precambrian basement that may originally have been part of the Tarim craton (Ma et al., 2012a,b, 2013, in press; Jian et al., 2013).

Supplementary data to this article can be found online at http://dx.doi.org/10.1016/j.gr.2013.09.005.

Acknowledgments

We thank A.K. Rybin, Director of the Research Station of the Russian Academy of Sciences in Bishkek for logistic support and hospitality during fieldwork. Chun Yang of the Beijing SHRIMP Centre prepared perfect zircon mounts and Ning Li and Liqin Zhou provided the zircon CL images. We appreciate the assistance of Alla Dolgopolova, Anton Kearsley and Chris Jones in the NMH laboratory. We also thank Zheng Xiang Li, Perth, for discussions on Tarim palaeogeography and Tao Wang, Yuruo Shi and Ying Tong, Beijing, for their help with the Chinese literature. Bor-ming Jahn, Stijn Glorie and an anonymous reviewer provided constructive comments leading the substantial improvements of the original manuscript. This study was supported by grants of the German Research Council (DFG) to YRA (RO7174/1-2) and AK (KR590/90-1) and RFBR Grants 11-05-91332 and 13-05-91151 to DVA. AKX and SAS acknowledge SPbSU grants 3.0.93.2010 and 3.37.91.2011. Y.R.-A. acknowledges the EU Framework Programme 7 funded SYNTHESYS Project at the Natural History Museum, London.

Appendix A. Analytical procedures

A.1. SHRIMP-II zircon dating procedures in Beijing and St. Petersburg

Zircon grains were hand-selected and mounted in epoxy resin together with chips of the M257 (Beijing) or Temora and 91500 (St. Petersburg) reference grains. The grains were sectioned approximately in half and polished. Reflected and transmitted light photomicrographs and cathodoluminescence (CL) SEM images (Hitachi S-3000N scanning electron microscope in the Beijing SHRIMP Centre; CamScan MX 2500S electron microscope with CL detector CLI/QUA 2 at VSEGEI, St. Petersburg) were prepared for all zircon grains. The CL images were used to decipher the internal structures of the sectioned grains and to target specific areas within the zircon crystals.

U–Pb analyses were made using identical SHRIMP-II instruments at the Beijing SHRIMP Centre, Chinese Academy of Geological Sciences, and the Centre of Isotopic Research, VSEGEI, St. Petersburg, Russia whose instrumental characteristics were described by De Laeter and Kennedy (1998). Each analysis consisted of 5 scans through the mass range. The spot diameter was about 25 μm in Beijing and 18 μm in St. Petersburg, and primary beam intensity was about 5–6 nA in Beijing and 4 nA in St. Petersburg. Analyses of samples and standards were alternated to allow assessment of Pb^+/U^+ discrimination. Raw data reduction and error assessment of the Beijing analyses followed the method described by Nelson (1997), using the Macintosh software programs Prawn 6.4, WALLEAD 2.7 and Plonk 4.3. The St. Petersburg data were reduced similar to the method described by Williams (1998, and references therein), using the SQUID Excel Macro of Ludwig (2000). The Pb/U ratios were normalized to the respective standards used in the two laboratories. Common-Pb corrections were applied using the ^{204}Pb-correction method, and because of very low counts on ^{204}Pb in most samples it was assumed that common lead was surface-related (Kinny, 1986). Uncertainties given for individual analyses (ratios and ages) are based on counting statistics and are given at the 1-σ level; uncertainties in pooled ages are reported at the 2-σ level.

A.2. LA-ICP-MS dating in London

Zircon mounts and CL images were prepared in the same manner as for SHRIMP analyses, and the grains were analyzed in the Department of Mineralogy, Natural History Museum, London, using an ESI New Wave UP193FX laser ablation system coupled to an Agilent 7500cs quadrupole-based ICP-MS. Samples and standard, mounted together, were ablated in an air-tight sample chamber flushed with either Ar or He for sample transport. The samples were rastered up and down lines, using a constant raster speed for each analysis. Data were collected in discrete runs of 20 analyses, comprising 12 unknowns bracketed before and after by 4 analyses of the standard zircon 91500 (Wiedenbeck et al., 1995). Data were collected for up to 180 s per analysis with a gas background taken during the initial ca. 60 s. Background and mass bias corrected signal intensities and counting statistics were calculated for each isotope. Concordia age calculations, weighted averages, intercept ages and plotting of concordia diagrams were performed using Isoplot/Ex rev. 2.49 (Ludwig, 2001). For each analysis, time-resolved signals were collected and then carefully studied to ensure that only flat stable signal intervals were included in the age calculations. The detailed analytical procedure is outlined in Jeffries et al. (2003).

A.3. LA-ICP-MS dating in Mainz

Zircon mounts and CL images were prepared in the same manner as for SHRIMP analyses, and the grains were analyzed in the Department of Geosciences, University of Mainz, using an Argilent 7500ce, coupled with a 213 nm New Wave UP213 Nd:YAG laser ablation system. Analyses were carried out with a beam diameter of 30 μm and a 10 Hz repetition rate. Ablation time was 30 s, resulting in pits ca. 30 μm deep. The standard zircon GJ-1 (Jackson et al., 2004) was used as a primary standard for correction of ^{207}Pb/^{235}U, ^{206}Pb/^{238}U and ^{208}Pb/^{232}Th ratios as well as for calculation of U and Th concentrations. Common Pb correction using ^{204}Pb could not be precisely determined with the quadrupole ICP-MS setups due to low count rates on ^{204}Pb in zircon and high background on ^{204}Hg. However, monitoring of ^{202}Hg and ^{204}(Hg + Pb) allowed calculation of minimum ^{206}Pb/^{204}Pb ratios. These ratios were not used for common Pb correction, but rather serve as a quality control, with ratios above 1000 considered to be insignificant compared to overall uncertainties. Off-line data reduction was performed by an in-house excel spreadsheet. Pooled ages were plotted and calculated using ISOPLOT/Excel version 3.6 (Ludwig, 2008). Accuracy of ^{207}Pb/^{235}U, ^{206}Pb/^{238}U and ^{208}Pb/^{232}Th ages was approx. 1.5%, based on long-term monitoring of several zircon standards (see Topuz et al., 2010). The results are presented in Table 5 where the isotopic ratios and ages are given with $1-\sigma$ error. Instrument parameters and further analytical details on U/Pb dating in Mainz are described in Zack et al. (2011).

A.4. LA-ICP-MS dating in Hong Kong

Zircon mounts and CL images were prepared in the same manner as for SHRIMP analyses, and the zircon grains were analyzed in the Department of Earth Sciences, University of Hong Kong, using a Nu Plasma HR MC-ICP-MS (Nu Instruments, UK), coupled with a 193 nm excimer laser ablation system (RESOlution M-50, Resonetics LLC, USA). Analyses were carried out with beam diameter of 40 μm and 5 Hz repetition rate. Instrument parameters and analytical details are described in Xia et al. (2011). Ablation time was 40 s, resulting in pits 30–40 μm deep. The standard zircons PL (Plesovice, Sláma et al., 2008) and GJ-1 (Jackson et al., 2004) were used for calibration. The instrument configuration does not allow to measure an internal element, so no U and Pb concentrations are given, but the Th/U ratio. Off-line data reduction was performed by the software ICPMSDataCal. Version 7.2 (Liu et al., 2010). Ages were calculated using ISOPLOT/Excel version 3.6 (Ludwig, 2008). The results are presented in Table x where the isotopic ratios and ages are given with 1-sigma errors.

Please cite this article as: Rojas-Agramonte, Y., et al., Detrital and igneous zircon ages for supracrustal rocks of the Kyrgyz Tianshan and palaeogeographic implications, Gondwana Research (2013), http://dx.doi.org/10.1016/j.gr.2013.09.005

A.5. LA-ICP-MS Hf-in-zircon isotopes in Beijing

Lu–Hf isotopic systematics was analyzed in the Institute of Geology and Geophysics, Chinese Academy of Sciences, Beijing, using a Thermo-Finnigan Neptune Plus Multi-Collector ICP-MS equipped with a Geolas-193 laser-ablation system. A laser repetition rate of 8 Hz at 20 J/cm^2 was used, and the spot size was 60 μm. Raw count rates for ^{172}Yb, ^{173}Yb, ^{175}Lu, ^{176}(Hf + Yb + Lu), ^{177}Hf, ^{178}Hf, ^{179}Hf, ^{180}Hf and ^{182}W were collected, and isobaric interference corrections for ^{176}Lu and ^{176}Yb on ^{176}Hf were determined. The ^{176}Yb/^{172}Yb value of 0.5887 and mean β_{Yb} value obtained during Hf analysis on the same spot were applied for the interference correction of ^{176}Yb on ^{176}Hf (Iizuka and Hirata, 2005). A ^{175}Lu/^{176}Lu value of 0.02655 and mean β_{Lu} value were used to calibrate the ^{176}Lu value and calculate the interference correction of ^{176}Lu on ^{176}Hf. The detailed analytical technique is described in Wu et al. (2006). During analyses, the ^{176}Hf/^{177}Hf ratios of the standards 91500 and GJ-1 were 0.282290 ± 30 (2 s.d., n = 26) and 0.282017 ± 34 (2 s.d., n = 25), respectively, similar to 0.282305 ± 8 (2 s.d., n = 111) and 0.281999 ± 8 (2 s.d., n = 10) measured using the solution method (Goolaerts et al., 2004; Woodhead et al., 2004; Wu et al., 2006).

References

Abdulin, A.A., Chimbulatov, M.A., Azerbaev, N.A., Ergaliev, G.Kh, Kasymov, M.A., Tsirel'son, B.S. (Eds.), 1986. Geology and metallogeny of Karatau, vol. 1. Alma-Ata (239 pp. (in Russian)).

Alexeiev, D.V., Ryazantsev, A.V., Kröner, A., Tretyakov, A.A., Xia, X., Liu, D.Y., 2011. Geochemical data and zircon ages for rocks in a high-pressure belt of Chu–Yili Mountains, southern Kazakhstan: implications for the earliest stages of accretion in Kazakhstan and the Tianshan. Journal of Asian Earth Sciences 42, 805–820.

An, F., Zhu, Y., Wei, S., Lai, S., 2013. An Early Devonian to Early Carboniferous volcanic arc in North Tianshan, NW China: geochronological and geochemical evidence from volcanic rocks. Journal of Asian Earth Sciences. http://dx.doi.org/10.1016/j.jseaes.2013.07.037 (in press).

Ankinovich, S.G., 1961. Lower Palaeozoic of the Vanadiferous basin of the North Tian-Shan and western margin of central Kazakhstan, Part 1. Academy of Sciences of Kazakh SSR.Alma-Ata (272 pp. (in Russian)).

Avdeev, A.V., Kovalev, A.A., 1989. Ophiolites and Evolution of the Southwestern Part of the Ural–Mongolia Folded Belt. Moscow University Publishing Co.(227 pp. (in Russian)).

Bakirov, A.B., 1978. Tectonic Position of Metamorphic Complexes in the Tian Shan. Ilim Publisher, Frunze (261 pp. (in Russian)).

Bakirov, A.B., Kotov, V.V., 1988. Eclogite-bearing metamorphic complexes as indicators of ancient continent collision zones. Precambrian and Lower Paleozoic of the Tian Shan. Ilim Publisher, Frunze, pp. 4–25 (in Russian).

Bakirov, A.B., Maksumova, R.A., 2001. Geodynamic evolution of the Tien Shan lithosphere. Russian Geology and Geophysics 42, 1359–1366.

Bakirov, A.B., Dobretsov, N.L., Lavrentiev, Yu.G., Usova, L.V., 1974. Eclogites of Atbashi Ridge, Tianshan. Doklady Earth Sciences 215, 677–680.

Bakirov, A.B., Tagiri, M., Sakiev, K., Ivleva, E.A., 2003. The Lower Precambrian rocks in the Tien Shan and their geodynamic setting. Geotectonics 37, 368–380.

Biske, Yu.S., 1995. Late Paleozoic collision of the Tarimskiy and Kirghiz–Kazakh paleocontinents. Geotectonics 29, 26–34.

Biske, Yu.S., 1996. Palaeozoic Structure and History of South Tian-Shan. St. Petersburg University Publishing House, St. Petersburg (192 pp. (in Russian)).

Biske, Yu.S., Zubtsov, Y.S., Porshnyakov, G.S., 1985. Hercynides of the Atbashi–Kokshaal Region of the Southern Tian-Shan. Leningrad State University Publishing House, Leningrad, USSR (190 pp. (in Russian)).

Biske, Yu.S., Alexeiev, D.V., Wang, B., Wang, F., Getman, O.F., Jenschuraeva, A.V., Seltmann, R., Aristov, V.A., 2012. Structures of the late Palaeozoic thrust belt in the Chinese South Tian Shan. Doklady Earth Sciences 442, 8–12.

Black, L.P., Kamo, S.L., Allen, C.M., Aleinikoff, J.N., Davis, D.W., Korsch, R.J., Foudoulis, C., 2003. TEMORA 1: a quality zircon standard for Phanerozoic U–Pb geochronology. Chemical Geology 200, 155–170.

Brookfield, M.E., 1994. Problems in applying preservation facies and sequence models to Sinian (Neoproterozoic) glacial sequences in Australia and Asia. Precambrian Research 70, 143–147.

Buslov, M.M., Saphonova, I.Yu., Watanabe, T., Obut, O.T., Fujiwara, Y., Iwata, K., Semakov, N.N., Sugai, Y., Smirnova, L.V., Kazansky, A.Yu., Itaya, T., 2001. Evolution of the Paleo-Asian Ocean (Altai-Sayan Region, Central Asia) and collision of possible Gondwana derived terranes with the southern marginal part of the Siberian continent. Geoscience Journal 5, 203–224.

Chakabaev, S.E. (Ed.), 1979. Geological Map of Kazakh SSR, scale 1:500,000, South Kazakhstan Series. Aerogeologiya, Leningrad (in Russian).

Charvet, J., Shu, L., Laurent-Charvet, S., 2007. Paleozoic structural and geodynamic evolution of eastern Tianshan (NW China): welding of the Tarim and Junggar plates. Episodes 30, 162–172.

Charvet, J., Shu, L., Laurent-Charvet, S., Wang, B., Faure, M., Cluzel, D., Chen, Y., De Jong, K., 2011. Palaeozoic tectonic evolution of the Tianshan belt, NW China. Science China Earth Sciences 54, 166–184.

Chumakov, N.M., 2009. The Baykonurian glaciohorizon of the late Vendian. Stratigraphy and Geological Correlation 17, 373–381.

Condie, K.C., Aster, R.C., 2010. Episodic zircon age spectra of orogenic granitoids: the supercontinent connection and continental growth. Precambrian Research 180, 227–236.

Cook, H.E., Taylor, M.E., Zhemchuzhnikov, V.G., Apollonov, M.K., Ergaliev, G.Kh, Sargaskayev, Zh.S, Dubinina, S.V., Mel'nikova, L.Yu, 1991. In: Cooper, J.D., Stevens, C.H. (Eds.), Comparison of Two Early Paleozoic Carbonate Submarine Fans, West United States and South Kazakhstan, Soviet Union. Paleozoic Paleogeography of the Western United States II Pacific Section SEPM, 67, pp. 847–872.

De Grave, J., Glorie, S., Buslov, M.M., Izmer, A., Fournier-Carrie, A., Batalev, V.Yu, Vanhaecke, F., Elburg, M., Van den haute, P., 2011. The thermo-tectonic history of the Song-Kul plateau, Kyrgyz Tien Shan: constraints by apatite and titanite thermochronometry and zircon U/Pb dating. Gondwana Research 20, 745–763.

De Grave, J., Glorie, S., Ryabinin, A., Zhimulev, F., Buslov, M.M., Izmer, A., Elburg, M., Vanhaecke, F., Van den haute, P., 2012. Late Palaeozoic and Meso-Cenozoic tectonic evolution of the southern Kyrgyz Tien Shan: constraints from multi-method thermochronology in the Trans-Alai, Turkestan-Alai segment and the southeastern Ferghana Basin. Journal of Asian Earth Sciences 44, 149–168.

De Grave, J., Glorie, S., Buslov, M.M., Stockli, D.F., McWilliams, M.O., Batalev, V.Yu., Van den haute, P., 2013. Thermo-tectonic history of the Issyk-Kul basement (Kyrgyz Northern Tien Shan, Central Asia). Gondwana Research 23, 998–1020.

De Laeter, J.R., Kennedy, A.K., 1998. A double focusing mass spectrometer for geochronology. International Journal of Mass Spectrometry 178, 43–50.

Degtyarev, K.E., Tolmacheva, T.Yu., Ryazantsev, A.V., Tret'yakov, A.A., Yakubchuk, A.S., Kotov, A.B., Sal'nikova, E.B., Yakivleva, S.Z., Gorokhovskii, B.M., 2012. Structure, age substantiation and tectonic setting of the Lower-Middle Ordovician volcanic-sedimentary and plutonic complexes of the western part of the Kyrgyz Range (Northern Tien Shan). Stratigraphy and Geological Correlation 20, 317–345.

Demoux, A., Kröner, A., Liu, D., Badarch, G., 2009. Precambrian crystalline basement in southern Mongolia as revealed by SHRIMP zircon dating. International Journal of Earth Sciences 98, 1365–1380.

Dobretsov, N.L., Buslov, M.M., 2007. Late Cambrian–Ordovician tectonics and geodynamics of Central Asia. Russian Geology and Geophysics 48, 71–82.

Gao, J., Long, L., Klemd, R., Qian, Q., Liou, D., Xiong, X., Su, W., Liu, W., Wang, Y., Yang, F., 2009. Tectonic evolution of the South Tianshan orogen and adjacent regions, NW China: geochemical and age constraints of granitoid rocks. International Journal of Earth Sciences 98, 1221–1238.

Ge, R., Zhu, W., Wu, H., Zheng, B., He, J., 2013. Timing and mechanisms of multiple episodes of migmatization in the Korla Complex; northern Tarim Craton; NW China: constraints from zircon U–Pb–Lu–Hf isotopes and implications for crustal growth. Precambrian Research 231, 136–156.

Ghes, M.D., 2008. Terrane Structure and Geodynamic Evolution of the Caledonides of the Tian Shan. Altyn Tamga Publishers, Bishkek (158 pp. (in Russian)).

Glorie, S., De Grave, J., Buslov, M.M., Elburg, M.A., Stockli, D.F., Van den haute, P., Gerdes, A., 2010. Multi-method chronometric constraints on the evolution of the northern Kyrgyz Tien Shan batholith: from emplacement to exhumation. Journal of Asian Earth Sciences 38, 131–146.

Glorie, S., De Grave, J., Buslov, M.M., Zhimulev, I., Stockli, D.F., Batalev, V.Y., Izmer, A., Van den haute, P., Vanhaecke, F., Elburg, M.A., 2011. Tectonic history of the Kyrgyz South Tien Shan (Atbashi–Inylchek) suture zone: the role of inherited structures during deformation–propagation. Tectonics 30, TC6016.

Goolaerts, A., Mattielli, N., de Jong, J., Weis, D., Scoates, J.S., 2004. Hf and Lu isotopic reference values for the zircon standard 91500 by MC-ICP-MS. Chemical Geology 206, 1–9.

Griffin, W.L., Pearson, N.J., Belousova, E., Jackson, S.E., van Achterbergh, E., O'Reilly, S.Y., Shee, S.R., 2000. The Hf isotope composition of cratonic mantle: LAM-MC-ICPMS analysis of zircon megacrysts in kimberlites. Geochimica et Cosmochimica Acta 64, 133–147.

Hall, R., Sevastjanova, I., 2012. Australian crust in Indonesia. Australian Journal of Earth Sciences 59, 827–844.

He, Z.-Y., Zhang, Z.-M., Zong, K.-Q., Dong, X., 2013. Paleoproterozoic crustal evolution of the Tarim craton: constrained by zircon U–Pb and Hf isotopes of meta-igneous rocks from Korla and Dunhuang. Journal of Asian Earth Sciences. http://dx.doi.org/10.1016/j.jseaes.2013.07.022 (in press).

Hegner, E., Klemd, R., Kröner, A., Corsini, M., Alexeiev, D.V., Iaccheri, L.M., Zack, T., Dulski, P., Xia, X., Windley, B.F., 2010. Mineral ages and P–T conditions of late Paleozoic high-pressure eclogite and provenance of mélange sediments in the South Tianshan Orogen of Kyrgyzstan. American Journal of Science 310, 916–950.

Huang, B.C., Xu, B., Zhang, C.X., Li, Y.A., Zhu, R.X., 2005. Paleomagnetism of the Baiyisi volcanic rocks (ca. 740 Ma) of Tarim, northwest China: a continental fragment of NeoproterozoicWestern Australia? Precambrian Research 142, 83–92.

Hynes, A., Rivers, T., 2010. Protracted continental collision — evidence from the Grenville orogen. Canadian Journal of Earth Sciences 47, 591–620.

Iizuka, T., Hirata, T., 2005. Improvements of precision and accuracy in in-situ Hf isotope microanalysis of zircon using the laser ablation-MC-ICPMS technique. Chemical Geology 220, 121–137.

Jackson, S.E., Pearson, N.J., Griffin, W.L., Belousova, E.A., 2004. The application of laser ablation inductively coupled plasma-mass spectrometry (LA–ICPMS) to in situ U–Pb zircon geochronology. Chemical Geology 211, 47–69.

Jeffries, T.E., Fernandez-Suarez, J., Corfu, F., Gutierrez Alonso, G., 2003. Advances in U–Pb geochronology using a frequency quintupled Nd:YAG based laser ablation system (l~213 nm) and quadrupole based ICP-MS. Journal of Analytical Atomic Spectrometry 18, 847–855.

Jian, P., Kröner, A., Jahn, B.-M., Liu, D., Zhang, W., Shi, Y., Ma, H., 2013. Zircon ages of metamorphic and magmatic rocks within peridotite-bearing mélanges: crucial time

Please cite this article as: Rojas-Agramonte, Y., et al., Detrital and igneous zircon ages for supracrustal rocks of the Kyrgyz Tianshan and palaeogeographic implications, Gondwana Research (2013), http://dx.doi.org/10.1016/j.gr.2013.09.005

constraints on early Carboniferous extensional tectonics in the Chinese Tianshan. Lithos 172–173, 243–266.
Khristov, Y.V., Mikolaichuk, A.V., 1983. Geosynclinal basement of the crust of the Fergana–Kokshaal Hercynides. Geotectonics 18, 233–241.
Khudoley, A.K., Semiletkin, S.A., 2008. The east margin of the Rheic Ocean: evidence from the latest Precambrian–early Paleozoic succession of the Talass Alatau–Karatau (Northern Tien-Shan, Kyrgyzstan). In: Keppie, J.D., Ramos-Arias, M., Morales-Gamez, M., Nance, R.D., Murphy, J.B., Keppie, D.F. (Eds.), The western End of the Rheic Ocean: Subduction Erosion Processes in Southern Mexico (IGCP Project No. 497). Guidebook and Abstracts, p. 47.
Kinny, P.D., 1986. 3820 Ma zircons from a tonalitic Amitsoq gneiss in the Godthab district of southern West Greenland. Earth and Planetary Science Letters 79, 337–347.
Kiselev, V.V., 1999. Uranium–Lead (on zircon) Geochronology of Magmatic Complexes of the North Tianshan. Izvestiya NAN KR Special Issue 21–33 (in Russian).
Kiselev, V.V., Korolev, V.G., 1972. Tectonics of the Precambrian of Middle Asia and Central Kazakhstan. Ilim Publishing House (79 pp. (in Russian)).
Kiselev, V.V., Zhukov, Yu.V., Israileva, R.M., Komarevtsev, V.T., Tsyganok, E.N., 1982. Radiological Evidence for the Grenville Tectono-Magmatic Stage in the Northern Tianshan. Izvestiya Academy of Sciences of the Kyrgyz SSR, 6 26–30 (in Russian).
Kiselev, V.V., Apayarov, F.Kh., Komartsev, V.T., Tsyganok, E.N., Lukashova, E.M., 1993. Isotopic ages of zircons from crystalline complexes of the Tianshan. In: Kozakov, I.K. (Ed.), Early Precambrian of the Central Asia Folded Belt. Nauka, St. Petersburg, pp. 99–115.
Konopelko, D., Biske, G., Seltmann, R., Eklund, O., Belyatsky, B., 2007. Hercynian post-, collisional A-type granites of the Kokshaal Range, Southern Tien Shan, Kyrgyzstan. Lithos 97, 140–160.
Konopelko, D., Biske, G., Seltmann, R., Kiseleva, M., Matukov, D., Sergeev, S., 2008. Deciphering Caledonian events: timing and geochemistry of the Caledonian magmatic arc in the Kyrgyz Tien Shan. Journal of Asian Earth Sciences 32, 131–141.
Konopelko, D., Seltmann, R., Biske, G., Lepekhina, E., Sergeev, S., 2009. Possible source dichotomy of contemporaneous post-collision barren I-type versus tin-bearing A-type granites, lying on opposite sides of the South Tien Shan suture. Ore Geology Reviews 35, 206–216.
Konopelko, D., Kullerud, K., Apayarov, F., Sakiev, K., Baruleva, O., Ravna, E., Lepekhina, E., 2012. SHRIMP zircon chronology of HP-UHP rocks of the Makbal metamorphic complex in the Northern Tien Shan, Kyrgyzstan. Gondwana Research 22, 300–309.
Korolev, V.G., Maksumova, R.A., 1984. Precambrian Tillite and Tilloids of the Tien Shan. Ilim Publisher, Frunze (190 pp. (in Russian)).
Kozakov, I.K., Sal'nikova, E.B., Wang, T., Didenko, A.N., Plotkina, Yu.V., Podkovyrov, 2007. Early Precambrian crystalline complexes of the Central Asian microcontinent: age, sources, tectonic position. Stratigraphy and Geological Correlation 15, 121–140.
Kröner, A., Windley, B.F., Badarch, G., Tomurtogoo, O., Hegner, E., Jahn, B.M., Gruschka, S., Khain, E.V., Demoux, A., Wingate, M.T.D., 2007. Accretionary growth and crust-formation in the Central Asian orogenic belt and comparison with the Arabian-Nubian shield. In: Hatcher, R.D., Carlson, M.P., McBride, J.H., Martínez Catalán, J.R. (Eds.), 4-D framework of continental crust. Geological Society of America, Memoir, 200, pp. 181–209.
Kröner, A., Hegner, E., Lehmann, B., Heinhorst, J., Wingate, M.T.D., Liu, D.Y., Ermelov, P., 2008. Palaeozoic arc magmatism in the Central Asian Orogenic Belt of Kazakhstan: SHRIMP zircon ages and whole-rock Nd isotopic systematics. Journal of Asian Earth Sciences 32, 118–130.
Kröner, A., Alexeiev, D.V., Hegner, E., Corsini, M., Mikolaichuk, A., Xia, X., Zack, T., Windley, B.F., Sun, M., Rojas-Agramonte, Y., Liu, D., 2009. New zircon, Sm–Nd, and Ar–Ar ages for Precambrian and Palaeozoic rocks from the Tianshan orogenic belt in Kyrgyzstan and disappearance of the Archaean. International Field Excursion and Workshop on Tectonic Evolution and Crustal Structure of the Paleozoic Chinese Tianshan, Urumqi, China, September 9–19, 2009, pp. 43–44.
Kröner, A., Alexeiev, D.V., Hegner, E., Rojas-Agramonte, Y., Corsini, M., Chao, Y., Wong, J., Windley, B.F., Liu, D., Tretyakov, A.A., 2012. Zircon and muscovite ages, geochemistry, and Nd–Hf isotopes for the Aktyuz metamorphic terrane: evidence for an Early Ordovician collisional belt in the northern Tianshan of Kyrgyzstan. Gondwana Research 21, 901–927.
Kröner, A., Alexeiev, D.V., Rojas-Agramonte, Y., Hegner, E., Wong, J., Xia, X., Belousova, E., Mikolaichuk, A., Seltmann, R., Liu, D., Kisilev, V., 2013. Mesoproterozoic (Grenville-age) terranes in the Kyrgyz North Tianshan: zircon ages and Nd–Hf isotopic constraints on the origin and evolution of basement blocks in the southern Central Asian Orogen. Gondwana Research 23, 272–295.
Kröner, A., Kovach, V., Belousova, E., Hegner, E., Armstrong, R., Dolgopolova, A., Seltmann, R., Alexeiev, D.V., Hoffmann, J.E., Wong, J., Sun, M., Cai, K., Wang, T., Tong, Y., Wilde, S.A., Degtyarev, K.E., Rytsk, E., 2013. Reassessment of continental growth during the accretionary history of the Central Asian Orogenic Belt. Gondwana Research 20 (in press).
Ksienszyk, A.K., Jacobs, J., Boger, S.D., Kosler, J., Sircombe, K.N., Whitehouse, M.J., 2012. U–Pb ages of metamorphic monazite and detrital zircon from the Northampton Complex: evidence of two orogenic cycles in Western Australia. Precambrian Research 198–199, 37–50.
Lei, R.X., Wu, C.Z., Gu, L.X., Zhang, Z.Z., Chi, G.X., Jiang, Y.H., 2011. Zircon U–Pb chronology and Hf isotope of the Xingxingxia granodiorite from the Central Tianshan zone (NW China): implications for the tectonic evolution of the southern Altaids. Gondwana Research 20, 582–593.
Lei, R.X., Wu, C.Z., Chi, G.X., Chen, G., Gu, L.X., Jiang, Y.H., 2012. Petrogenesis of the Palaeoproterozoic Xishankou pluton, northern Tarim block, northwest China: implications for assembly of the supercontinent Columbia. International Geology Review.
Lei, R.-X., Wu, C.-Z., Chi, G.-X., Gu, L.-X., Dong, L.-H., Qu, X., Jiang, Y.-H., Jiang, S.-Y., 2013. The Neoproterozoic Hongliujing A-type granite in Central Tianshan (NW China): LA-ICP-MS zircon U–Pb geochronology, geochemistry, Nd–Hf isotope and tectonic significance. Journal of Asian Earth Sciences 74, 142–154.
Levashova, N.M., Meert, J.G., Gibsher, A.S., Grice, W.C., Bazheniv, M.L., 2011. The origin of microcontinents in the Central Asian Orogenic Belt: constraints from paleomagnetism and geochronology. Precambrian Research 185, 37–54.
Li, S.W., Xu, D.K. (Eds.), 2007. Geological map of Chinese Tianshan and adjacent areas, scale 1:1000000. Beijing, Geology Publishing House. 2 sheets (in Chinese).
Li, Z.X., Zhang, L., Powell, McA, 1996. Positions of the East Asian cratons in the Neoproterozoic supercontinent Rodinia. Australian Journal of Earth Sciences 43, 593–604.
Li, H.M., Lu, S.N., Zheng, J.K., 2001. Dating of 3.6 Ga zircon in granite gneiss from the eastern Altyn Mountain and its geological significance. Bulletin of Mineralogy, Petrology and Geochemistry 20, 259–262 (in Chinese).
Li, Z.X., Bogdanova, S.V., Collins, A.S., Davidson, A., De Waele, B., Ernst, R.E., Fitzsimons, I.C.W., Fuck, R.A., Gladkochub, D.P., Jacobs, J., Karlstrom, K.E., Lu, S., Natapov, L.M., Pease, V., Pisarevsky, S.A., Thrane, K., Vernikovsky, V., 2008. Assembly, configuration, and break-up history of Rodinia: a synthesis. Precambrian Research 160, 179–210.
Li, Z.X., Evans, D.A.D., Halverson, G., 2013. Neoproterozoic glaciations in a revised global palaeogeography from the breakup of Rodinia to the assembly of Gondwana land. Sedimentary Geology 294, 219–232.
Liu, S.W., Guo, Z.J., Zhang, Z.C., Li, Q.G., Zheng, H.F., 2004. Nature of the Precambrian metamorphic blocks in the eastern segment of Central Tianshan: constraints from geochronology and Nd isotopic geochemistry. Science in China (Series D: Earth Sciences) 47, 1085–1094.
Liu, Y., Gao, S., Hu, Z., Gao, C., Zong, K., Wang, D., 2010. Continental and oceanic crust recycling-induced melt–peridotite interactions in the Trans-North China Orogen: U–Pb dating, Hf isotopes and trace elements in zircons from mantle xenoliths. Journal of Petrology 51, 537–571.
Lomize, M.G., Demina, L.I., Zarshchicov, A.V., 1997. The Kyrgyz–Terskei paleoceanic basin in the Tien Shan. Geotectonics 31, 463–482.
Long, X., Yuan, C., Sun, M., Kröner, A., Zhao, G., Wilde, S., Hu, A., 2011. Reworking of the Tarim Craton by underplating of mantle plume-derived magmas: evidence from Neoproterozoic granitoids in the Kuluketage area, NW China. Precambrian Research 187, 1–14.
Lu, S., Li, H., Zhang, C., Niu, G., 2008. Geological and geochronological evidence for the Precambrian evolution of the Tarim Craton and surrounding continental fragments. Precambrian Research 160, 94–107.
Ludwig, K.R., 2000. SQUID 1.00, A User's Manual. Special Publication, no. 2. Berkeley Geochronology Center, Berkeley, USA.
Ludwig, K.R., 2001. Isoplot/Ex version 2.49. Special Publication, 1a. Berkeley Geochronology Center (55 pp.).
Ludwig, K., 2008. Users Manual for ISOPLOT 3.6: A Geochronological Toolkit for Microsoft Excel. Special Publication, 4. Berkeley Geochronology Center, University of California at Berkeley ((revision of April 8, 2008), 77 pp.).
Luo, F.Z., 1989. On Precambrian of Mid-Tianshan uplift (metamorphic) zone. Xinjiang Geology 7, 24–33 (in Chinese).
Ma, X., Shu, L., Santosh, M., Li, J., 2012a. Detrital zircon U–Pb geochronology and Hf isotope data from Central Tianshan suggesting a link with the Tarim Block: implications on Proterozoic supercontinent history. Precambrian Research 206–207, 1–16.
Ma, X., Shu, L., Jahn, B.-M., Zhu, W., Faure, M., 2012b. Precambrian tectonic evolution of Central Tianshan, NW China: constraints from U–Pb dating and in situ Hf isotopic analysis of detrital zircons. Precambrian Research 222–223, 450–473.
Ma, X., Shu, L., Santosh, M., Li, J., 2013. Paleoproterozoic collisional orogeny in Central Tianshan: assembling the Tarim Block within the Columbia supercontinent. Precambrian Research 228, 1–19.
Ma, X., Shu, L., Meert, J.G., Li, J., 2013. The Paleozoic evolution of Central Tianshan: geochemical and geochronological evidence. Gondwana Research. http://dx.doi.org/10.1016/j.gr.2013.05.015 (in press).
Maksumova, R.A., Dzhenchuraeva, A.V., Berezanskii, A.V., 2001. Structure and evolution of the Tien Shan nappe-folded orogen. Russian Geology and Geophysics 42, 1367–1374.
Meert, J.G., Gibsher, A.S., Levashova, N.M., Grice, W.C., Kamenov, G.D., Ryabinin, A.B., 2011. Glaciation and 770 Ma Ediacara (?) fossils from the Lesser Karatau microcontinent, Kazakhstan. Gondwana Research 19, 867–880.
Metcalfe, I., 2011. Tectonic framework and Phanerozoic evolution of Sundaland. Gondwana Research 19, 3–21.
Mikolaichuk A.V., Buchroithner A. (Eds.), 2008. Geological map of the Khan-Tengri Massif. Scale 1:200 000/ISTC Project KR-920. http://www.cluster.istc.kg.
Mikolaichuk, A.V., Kurenkov, S.A., Degtyarev, K.E., Rubtsov, V.I., 1997. Northern Tien-Shan, main stages of geodynamic evolution in the late Precambrian and early Palaeozoic. Geotectonics 31, 445–462.
Mitrofanov, F.P. (Ed.), 1982. The Precambrian of Middle Asia. Nauka Publishing House, Leningrad (264 pp. (in Russian)).
Mossakovsky, A., Ruzhentsev, S., Samygin, S., Kheraskova, T., 1993. Central Asian fold belt: geodynamic evolution and history of formation. Geotectonics 6, 3–33.
Neievin, A.V., Biske, Yu.S., Neievin, I.A., 2011. Lower Palaeozoic Stratigraphy of the Syrdariya Continental Massif in the Eastern Part of the Middle Tianshan in Connection with Questions of Palaeogeography and Geodynamics. "Vestnik" of Sankt-Petersburg State University, Series 7, 2, pp. 21–36 (in Russian).
Nelson, D.R., 1997. Compilation of SHRIMP U–Pb zircon geochronology data, 1996. Geological Survey of Western Australia, Record 1997, 2 189.
Nikolaev, V.A., 1933. About Principal Structural Line of Tian Shan. Proceedings of All-Russian Mineralogical Society, Series 2, Part 62, 2, pp. 347–354 (in Russian).

Please cite this article as: Rojas-Agramonte, Y., et al., Detrital and igneous zircon ages for supracrustal rocks of the Kyrgyz Tianshan and palaeogeographic implications, Gondwana Research (2013), http://dx.doi.org/10.1016/j.gr.2013.09.005

Osmonbetov, K.O., 1980. Geological map of the Kyrgyz SSR, scale 1:500000. VSEGEI, Leningrad (in Russian).
Osmonbetov, K.O., Knauf, V.I., Korolev, V.T. (Eds.), 1982. Stratified and Intrusive Formations of Kyrgyzia, 1. Ilim Publishing House, Frunze (357 pp. (in Russian)).
Popov, V.I., 1938. History of Depressions and Uplifts of the West Tian Shan. Com. Nauk USSR, Tashkent (415 pp. (in Russian)).
Rojas-Agramonte, Y., Kröner, A., Demoux, A., Xia, X., Wang, W., Donskaya, T., Liu, D., Sun, M., 2011. Detrital and xenocrystic zircon ages from Neoproterozoic to Palaeozoic arc terranes of Mongolia: significance for the origin of crustal fragments in the Central Asian Orogenic Belt. Gondwana Research 19, 751–763.
Rojas-Agramonte, Y., Herwartz, D., García-Casco, A., Kröner, A., Alexeiev, D.V., Klemd, R., Buhre, S., Barth, M., 2013. Early Palaeozoic deep subduction of continental crust in the Kyrgyz North Tianshan: evidence from Lu–Hf garnet geochronology and petrology of mafic dykes. Contributions to Mineralogy and Petrology 166, 525–543.
Rytsk, E.Yu., Kovach, V.P., Yarmolyuk, V.V., Kovalenko, V.I., Bogomolov, E.S., Kotov, A.B., 2011. Isotopic structure and evolution of the continental crust in the East Transbaikalian segment of the Central Asian Foldbelt. Geotectonics 45, 349–377.
Seltmann, R., Konopelko, D., Biske, G., Divaev, F., Sergeev, S., 2011. Hercynian post-collisional magmatism in the context of Paleozoic magmatic evolution of the Tien Shan orogenic belt. Journal of Asian Earth Sciences 42, 821–838.
Shayakubov, T.Sh. (Ed.), 1998. Geological map of Uzbekistan, scale 1:500000. Tashkent, Cartographic Centre (in Russian).
Shields, G.A., 2008. Palaeoclimate: Marinoan meltdown. Nature Geoscience 1, 351–353.
Shu, L.S., Yu, J.H., Charvet, J., Laurent-Charvet, S., Sang, H.Q., Zhang, R.G., 2004. Geological, geochronological and geochemical features of granulites in the Eastern Tianshan, NW China. Journal of Asian Earth Sciences 24, 25–41.
Shu, L.S., Deng, X.L., Zhu, W.B., Ma, D.S., Xiao, W.J., 2011. Precambrian tectonic evolution of the Tarim Block, NW China: new geochronological insights from the Quruqtagh domain. Journal of Asian Earth Sciences 42, 774–790.
Sircombe, K.N., 1999. Tracing provenance through the isotope ages of littoral and sedimentary detrital zircon, eastern Australia. Sedimentary Geology 124, 47–67.
Sláma, J., Kosler, J., Condon, D.J., Crowley, J.L., Gerdes, A., Hanchar, J.M., Horstwood, M.S.A., Morris, G.A., Nasdala, L., Norberg, N., Schaltegger, U., Schoene, B., Tubrett, M.N., Whitehouse, M.J., 2008. Plesovice zircon — a new natural standard for U–Pb and Hf isotopic microanalysis. Chemical Geology 249, 1–35.
Tursungaziev, B.T., Petrov, O.V. (Eds.), 2008. Geological map of the Kyrghyz Republic. VSEGEI, St.-Petersburg, scale 1:500.000 (in Russian).
Voice, P.J., Kowalewski, M., Eriksson, K.A., 2012. Quantifying the timing and rate of crustal evolution: global compilation of radiometrically dated detrital zircon grains. Journal of Geology 119, 109–126.
Voitenko, V.N., Khudoley, A.K., 2012. Structural evolution of metamorphic rocks in the Talas Alatau, Tien Shan, Central Asia: implication for early stages of the Talas–Ferghana Fault evolution. Comptes Rendus Geosciences 344, 138–148.
Wang, B., Faure, M., Shu, L.S., Cluzel, D., Chen, Y., 2008. Paleozoic geodynamic evolution of the Yili Block, Western Chinese Tianshan. Bulletin de la Société Géologique de France 179, 483–490.
Wang, Z.-M., Han, C.-M., Su, B.-X., Sakyi, P.A., Malaviarachchi, S.P.K., Ao, S.-J., Wang, L.-J., 2013. The metasedimentary rocks from the eastern margin of the Tarim Craton: petrology, geochemistry, zircon U–Pb dating, Hf isotopes and tectonic implications. Lithos 179, 120–136.
Wiedenbeck, M., Allé, P., Corfu, F., Griffin, W.L., Meier, M., Oberli, F., von Quadt, A., Roddick, J.C., Spiegel, W., 1995. Three natural zircon standards for U–Th–Pb, Lu–Hf, trace element and REE analyses. Geostandards Newsletter 19, 1–23.
Williams, I.S., 1998. U–Th–Pb geochronology by ion microprobe. In: McKibben, M.A., Shanks III, W.C., Ridley, W.I. (Eds.), Applications of Microanalytical Techniques to Understanding Mineralizing Processes. Reviews in Economic Geology, 7, pp. 1–35.
Windley, B.F., Alexeiev, D.V., Xiao, W., Kröner, A., Badarch, G., 2007. Tectonic models for accretion of the Central Asian Orogenic Belt. Journal of the Geological Society of London 164, 31–47.
Woodhead, J., Hergt, J., Shelley, M., Eggins, S., Kemp, R., 2004. Zircon Hf-isotope analysis with an excimer laser, depth profiling, ablation of complex geometries, and concomitant age estimation. Chemical Geology 209, 121–135.
Wu, F.Y., Yang, Y.H., Xie, L.W., Yang, J.H., Xu, P., 2006. Hf isotopic compositions of the standard zircons in U–Pb geochronology. Chemical Geology 234, 105–126.
Xia, X.P., Sun, M., Sun, Y.L., Wang, Y.J., Zhao, G.C., 2011. Quasi-simultaneous determination of U–Pb and Hf isotope compositions of zircon by excimer laser-ablation multiple-collector ICPMS. Journal of Analytical Atomic Spectrometry 26, 1868–1871.
Xiao, S., Bao, H., Wang, H., Kaufmann, A.J., Zhou, C., Li, G., Yuan, X., Ling, H., 2004. The Neoproterozoic Quruqtagh Group in eastern Chinese Tianshan: evidence for a post-Marinoan glaciation. Precambrian Research 130, 1–26.
Xiao, W., Windley, B.F., Allen, M.B., Han, C., 2013. Paleozoic multiple accretionary and collisional tectonics of the Chinese Tianshan orogenic collage. Gondwana Research 23, 1316–1341.
Xu, B., Xiao, S., Zou, H., Chen, Y., Li, Z.-X., Song, B., Liu, D., Zhou, C., Yuan, X., 2009. SHRIMP zircon U–Pb age constraints on Neoproterozoic Quruqtagh diamictites in NW China. Precambrian Research 168, 247–258.
Xu, Z.-Q., He, B.-Z., Zhang, C.-L., Zhang, J.-X., Wang, Z.-M., Cai, Z.-H., 2013. Tectonic framework and crustal evolution of the Precambrian basement of the Tarim Block in NW China: new geochronological evidence from deep drilling samples. Precambrian Research 235, 150–162.
Yang, H.B., Gao, P., Li, B., Zhang, Q.J., 2005. The geological character of the Sinian Dalubayi ophiolite in the west Tianshan, Xinjiang. Xinjiang Geology 23, 123–126 (in Chinese with English abstract).
Zack, T., Stockli, D.F., Luvizotto, G.L., Barth, M.G., Belousova, E., Wolfe, M.R., Hinton, R.W., 2011. In situ U–Pb rutile dating by LA-ICP-MS: ^{208}Pb correction and prospects for geological applications. Contributions to Mineralogy and Petrology 162, 515–530.
Zhan, S., Chen, Y., Xu, B., Wang, B., Faure, M., 2007. Late Neoproterozoic paleomagnetic results from the Sugetbrak Formation of the Aksu area, Tarim basin (NW China) and their implications to paleogeographic reconstructions and the snowball Earth hypothesis. Precambrian Research 154, 143–158.
Zhang, C.-L., Zou, H.-B., Li, H.-K., Wang, H.-Y., 2013. Tectonic framework and evolution of the Tarim Block in NW China. Gondwana Research 23, 1306–1315.
Zhu, W.B., Zhang, Z.Z., Shu, L.S., Lu, H.F., Sun, J.B., Yang, W., 2008. SHRIMP U–Pb zircon geochronology of Neoproterozoic Korla mafic dykes in the northern Tarim Block, NW China: implications for the long-lasting breakup process of Rodinia. Journal of the Geological Society 165, 887–890.
Zhu, W.B., Zheng, B.H., Shu, L.S., Ma, D.S., Wan, J.L., Zheng, D.W., Zhang, Z.Y., Zhu, X.Q., 2011a. Geochemistry and SHRIMP U–Pb zircon geochronology of the Korla mafic dykes: constrains on the Neoproterozoic continental breakup in the Tarim Block, northwest China. Journal of Asian Earth Sciences 42, 791–804.
Zhu, W.B., Zheng, B.H., Shu, L.S., Ma, D.S., Wu, H.L., Li, Y.X., Huang, W.T., Yu, J.J., 2011b. Neoproterozoic tectonic evolution of the Precambrian Aksu blueschist terrane, northwestern Tarim, China: insights from LA-ICP-MS zircon U–Pb ages and geochemical data. Precambrian Research 185, 215–230.

Please cite this article as: Rojas-Agramonte, Y., et al., Detrital and igneous zircon ages for supracrustal rocks of the Kyrgyz Tianshan and palaeogeographic implications, Gondwana Research (2013), http://dx.doi.org/10.1016/j.gr.2013.09.005